

GIV/Girdin binds BRCA1 and links trimeric G-proteins to DNA damage response

Authors: Amer Ali Abd El-Hafeez^{1,†}, Nina Sun¹, Anirban Chakraborty², Jason Ear^{1,3}, Suchismita Roy¹, Pranavi Chamarthi¹, Navin Rajapakse¹, Soumita Das⁴, Kathryn E. Luker⁵, Tapas K. Hazra², Gary D. Luker⁵⁻⁷, Pradipta Ghosh^{1, 8-10§}

Affiliations:

¹Department of Cellular and Molecular Medicine, University of California San Diego, La Jolla, California 92093, USA

²Department of Internal Medicine, University of Texas Medical Branch, Galveston, Texas 77555, USA

³Biological Sciences Department, California State Polytechnic University, Pomona, California 91768, USA

⁴Department of Pathology, University of California San Diego, La Jolla, California 92093, USA

⁵Center for Molecular Imaging, Department of Radiology, University of Michigan 109 Zina Pitcher Place, Ann Arbor, MI, 48109-2200, USA

⁶Department of Biomedical Engineering, University of Michigan, , 2200 Bonisteel, Blvd., Ann Arbor, MI, 48109-2099, USA.

⁷Department of Microbiology and Immunology, University of Michigan, , 109 Zina Pitcher Place, Ann Arbor, MI, 48109-2200, USA

⁸Department of Medicine, University of California San Diego, La Jolla, California 92093, USA

⁹Moore's Comprehensive Cancer Center, University of California San Diego, La Jolla, California 92093, USA

¹⁰Veterans Affairs Medical Center, La Jolla, CA, USA.

[†]**Secondary Affiliation:** Pharmacology and Experimental Oncology Unit, Cancer Biology Department, National Cancer Institute, Cairo University, Cairo, Egypt

*Corresponding author:

Pradipta Ghosh, M.D.; Professor of Medicine and Cell and Molecular Medicine, University of California San Diego; 9500 Gilman Drive (MC 0651), George E. Palade Bldg, Rm 331-333; La Jolla, CA 92093.

Phone: 858-822-7633; **Fax:** 858-822-7636; **Email:** prghosh@health.ucsd.edu

Classification: BIOLOGICAL SCIENCES; Cell Biology

Key Words: Heterotrimeric G proteins, Guanine-nucleotide exchange modulators (GEMs), Non-receptor G protein signaling, CCDC88A, Akt

Word Count:

Cover page:

Abstract: 165

Significance: 113

Introduction: 640

Results, Discussion, Conclusions: 4869

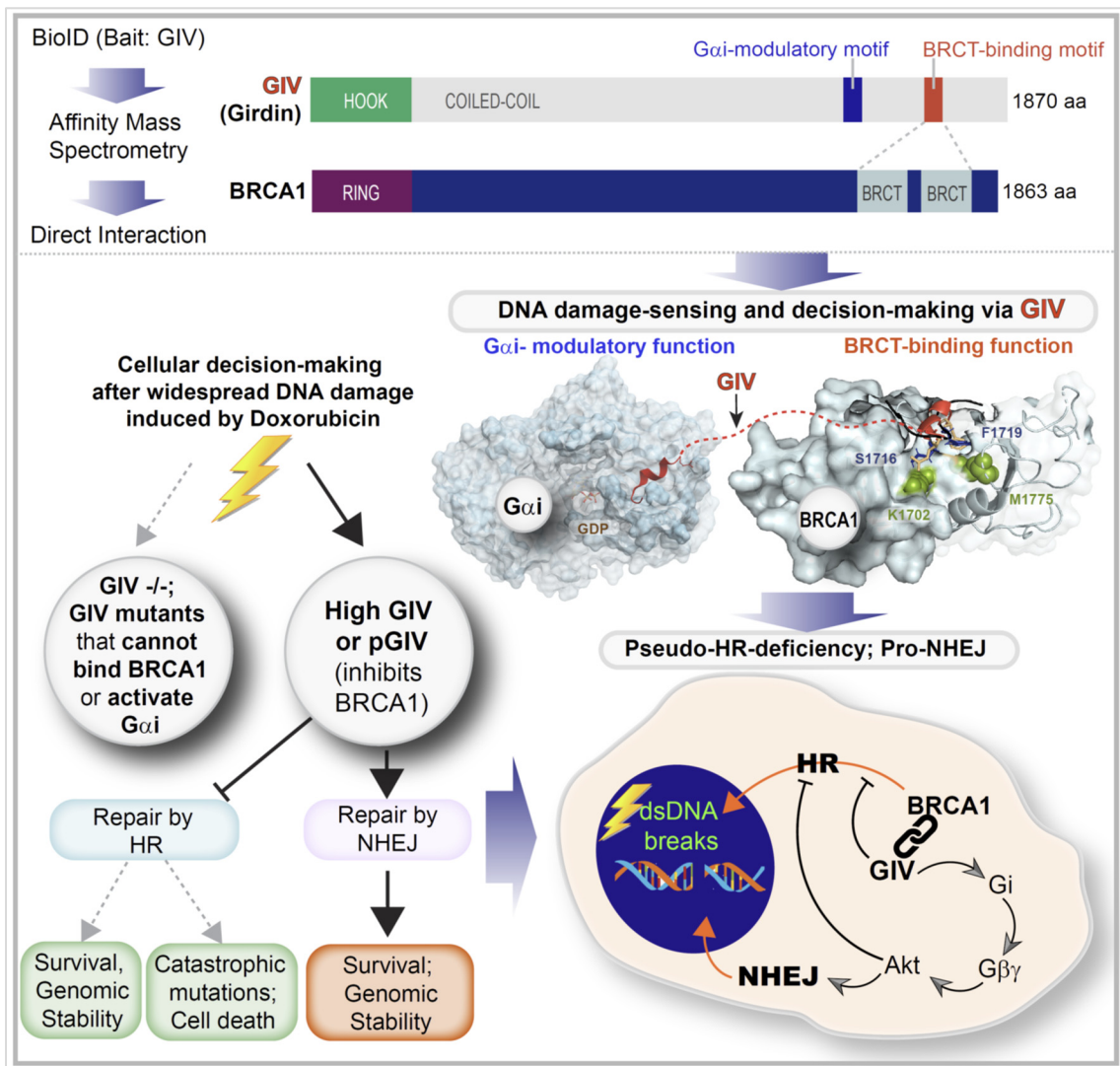
Materials and Methods: 61

Acknowledgements: 92

Figure Legends: 2009

Total: 7949

54 **GRAPHIC ABSTRACT:**



88

89 **HIGHLIGHTS:**

- 90
- 91
- 92
- 93
- 94
- Non-receptor G protein modulator, GIV/Girdin binds BRCA1
 - Binding occurs in both canonical and non-canonical modes
 - GIV sequesters BRCA1 away from dsDNA breaks, suppresses HR
 - Activation of Gi by GIV enhances Akt signals, favors NHEJ

95 **IN BRIEF:**

96 In this work, the authors show that heterotrimeric G protein signaling that is triggered by non-receptor

97 GEF, GIV/Girdin, in response to double-stranded DNA breaks is critical for decisive signaling events

98 which favor non-homologous end-joining (NHEJ) and inhibit homologous recombination (HR).

99

100 **Summary (165 words)**

101
102 Upon sensing DNA double-strand breaks (DSBs), eukaryotic cells either die or repair DSBs *via* one of two
103 competing pathways, i.e., non-homologous end-joining (NHEJ) or homologous recombination (HR). We show
104 that cell fate after DNA damage hinges on two functions of GIV/Girdin, a guanine nucleotide-exchange modulator
105 of heterotrimeric G-protein, $G_{i\alpha}\beta\gamma$. First, GIV suppresses HR by binding and sequestering BRCA1, a key
106 coordinator of multiple steps within the HR pathway, away from DSBs; it does so using a C-terminal motif that
107 binds BRCA1's BRCT-modules *via* both phospho-dependent and -independent mechanisms. Second, GIV
108 promotes NHEJ, and binds and activates G_i and enhances the 'free' $G\beta\gamma \rightarrow PI-3\text{-kinase} \rightarrow Akt$ pathway, thus
109 revealing the enigmatic origin of pro-survival Akt signals during dsDNA repair. Absence of GIV, or the loss of
110 either of its two functions impaired DNA repair, and induced cell death when challenged with numerous cytotoxic
111 agents. That GIV selectively binds few other BRCT-containing proteins suggests convergent signaling such that
112 heterotrimeric G-proteins may finetune sensing, repair, and outcome after DNA damage.

113
114
115
116
117
118
119
120
121
122
123
124
125
126
127
128
129
130
131
132
133
134
135
136
137
138
139
140
141
142
143
144
145

146 **Significance Statement (113 words)**

147
148 To tide of any stress, temporospatially segregated signaling pathways in cells are often scaffolded to generate
149 cooperativity between unlikely pathways. Here we report such an unexpected crosstalk that is orchestrated *via*
150 a non-receptor multimodular G protein activator, GIV/Girdin, which decisively skews the functions of BRCA1 and
151 the choice of cellular responses after DNA damage. GIV binds and sequesters BRCA1 away from dsDNA breaks,
152 suppressing HR. In addition, activation of trimeric Gi by GIV enhances Akt signals, favoring NHEJ. These findings
153 reveal a hitherto unknown link between a major hub in DNA repair (i.e., BRCA1) and a signaling hub of
154 paramount importance in essentially all aspects of modern medicine (i.e., trimeric G proteins).

155 Introduction

156 Genomic integrity is under constant attack from extrinsic and intrinsic factors that induce DNA damage (1).
157 Damaged DNA must be repaired to maintain genomic integrity *via* processes that are personalized and evolved
158 by the cell type, collectively termed as the DNA damage response (DDR) (2). DDRs are orchestrated by an
159 incredibly complex network of proteins that sense and assess the type and extent of damage, decide between
160 cell fates (death vs. repair), choose a repair pathway, and then initiate and complete the repair process (3). For
161 example, the DDR involves the activation of ATM kinase, a member of the phosphoinositide 3-kinase (PI3K)-
162 related protein kinase family (4) which is rapidly recruited by the MRE11-RAD50-NBS1 (MRN) complex to
163 chromatin (5). Phosphorylation of a large number of substrates follows, which in turn activates cell cycle
164 checkpoints and triggers the recruitment of repair factors to the DSBs. Positive feedback loops are orchestrated
165 to amplify the signals, e.g., ATM phosphorylates the histone variant H2AX (resulting in the formation of the
166 phosphorylated form called γ H2AX) (6), which recruits additional ATM molecules and further accumulation of
167 γ H2AX (7-9).

168 Among the types of DNA damage, DNA double-strand breaks (DSBs) are the most cytotoxic lesions that
169 threaten genomic integrity (10). Failure to repair DSBs results in genomic instability and cell death. DNA repair
170 can be achieved by different means that are commonly grouped into two broad, competing categories (11):
171 homologous recombination (HR) and non-homologous end joining (NHEJ) (12). HR, which requires a
172 homologous template to direct DNA repair, is generally believed to be a high-fidelity pathway (13). By contrast,
173 NHEJ directly seals broken ends; while some believe that repair by NHEJ is imprecise, we have shown that
174 precision can indeed be achieved (14). In fact, NHEJ offers an ideal balance of flexibility and accuracy when the
175 damage to DNA is widespread with DSBs featuring diverse end structures (15). Consequently, it is believed to
176 represent the simplest and fastest mechanism to heal DSBs (16), thus it is the most predominant DSB repair
177 pathway within the majority of mammalian cells. Key molecular players in both pathways have been identified:
178 53BP1, first identified as a DNA damage checkpoint protein, and Breast cancer type 1 susceptibility
179 protein (BRCA1), a well-known breast cancer tumor suppressor (17), are at the center of molecular networks
180 that coordinate NHEJ and HR, respectively.

181 How the choice of DSB repair pathway is determined at a molecular level has been the subject of intense
182 study for a decade (18,19). Here we reveal a previously unforeseen determinant of the choice of DNA damage,
183 GIV (Girdin), which is a non-receptor activator of heterotrimeric (henceforth, trimeric) G-protein, Gi (20,21).
184 Trimeric G-proteins are a major signaling hub in eukaryotes that gate signaling downstream of 7-transmembrane
185 (7TM)-receptors called GPCRs, and the GPCR/G-protein pathway is of paramount importance in modern
186 medicine, serving as a target of about 34% of marketed drugs (22). Although peripheral players in the GPCR/G-
187 protein pathway have been found to have indirect impact on DDR [reviewed in (23)], the role of G-proteins in
188 DDR has never been established. Unlike GPCRs that primarily sense the exterior of the cell, GIV-GEM the
189 prototypical member of a family of cytosolic guanine-nucleotide exchange modulators (GEMs), senses and

190 coordinates cellular response to intracellular events (e.g., autophagy, ER-stress, unfolded protein response,
191 inside-out signaling during mechanosensing, etc) by activating endomembrane localized GTPases (24,25). By
192 virtue of its ability to coordinate multiple cellular processes, many of which impart aggressive traits to tumor cells,
193 GIV has emerged as a *bona-fide* oncogene that supports sinister properties of cancer cells, favors aggressive
194 tumor phenotypes in diverse types of cancers, and drives poor survival outcomes [reviewed in (26)]. We provide
195 mechanistic insights into how GIV-GEM inhibits HR and concomitantly enhances NHEJ. In doing so, this work
196 not only reveals another pro-tumorigenic role of GIV, but also begins to unravel how endomembrane G-protein
197 signaling shapes decision-making during DDR.

201 **Results and Discussion**

202 ***Proteomic studies suggest a putative role for GIV during DNA damage response***

203 The interactome of a protein dictates its localization and cellular functions. To map the landscape of GIV's
204 interactome we carried out proximity-dependent biotin identification (BioID) coupled with mass spectrometry
205 (MS) (**Fig 1A**). BirA-tagged GIV construct was validated by immunoblotting and found to be expressed in cells
206 as full-length proteins of expected molecular size (~250 kDa) (**Fig 1B**). Samples were subsequently processed
207 for protein identification by Mass Spectrometry. Gene ontology (GO) cellular component analysis, as determined
208 by DAVID GO, revealed that GIV-proximal interactors were in both cytoplasmic and nuclear compartments (**Fig**
209 **1C**; See **Extended Data 1**); one interactor (i.e., BRCA1) was predicted to bind GIV across three different cellular
210 compartments (**Fig 1C**; red bars). GO-molecular function analysis revealed that "DNA binding proteins" was the
211 most enriched class of proteins in GIV's interactome (**Fig 1D**; **Extended Data 2**). BRCA1 was a notable interactor
212 within that class, and the serine/threonine-specific protein kinase, Ataxia telangiectasia and Rad3 related protein
213 (ATR), that coordinates DNA damage sensing and repair was another (**Fig 1E**). A reactome pathway analysis of
214 DNA-binding proteins in the GIV's interactome showed that GIV's interactome enrichment for proteins that
215 participate in gene transcription, regulation of cell cycle, and in DNA repair (**Fig 1E-F**). These findings were rather
216 surprising because GIV's presence on nuclear speckles was described almost a decade ago (27), and yet,
217 among all the functions of GIV that have emerged since its discovery in 2005, little to nothing is known about
218 GIV's role in sensing/signaling during intranuclear processes.

220 ***GIV is required for DNA damage response***

221 We generated HeLa cells without GIV using CRISPR Cas9 and subsequently exposed them to Doxorubicin
222 followed by several commonly used readouts of DDR (**Fig 2A**; **S1A-B**). A mixture of -/- (henceforth, GIV KO)
223 clones were pooled to recapitulate the clonal heterogeneity of parental HeLa cells (**Fig S1B**), and near-complete
224 depletion of GIV (estimated ~95% by band densitometry) was confirmed by immunoblotting (**Fig 2B**). We chose

225 HeLa cells because DDR has been extensively studied in this cell line (28,29) and because HeLa cells have
226 defective p53 (30). The latter is relevant because GIV/CCDC88A aberrations (gene amplification) co-occur with
227 defects in the tumor suppressor TP53 (TCGA pancancer profile; cbiportal.org); ~36% of tumors with aberrant
228 CCDC88A expression was also associated with mis-sense and truncating driver mutations in TP53. We chose
229 Doxorubicin (henceforth, Dox) for inducing DNA damage because it is a widely used anthracycline anticancer
230 agent and its impact on DNA integrity in HeLa cells has been mapped for each cell cycle with demonstrated
231 reproducibility (31). Compared to parental cells, fewer metabolically active GIV KO cells survived after a Dox
232 challenge, as determined using a MTT assay (**Fig 2C; Fig S1C**), indicating that in the absence of GIV, cells
233 show markedly reduced survival from cytotoxic lesions induced by Dox. GIV KO cells showed increased
234 susceptibility also to two other cytotoxic drugs, Cisplatin and Etoposide (**Fig S1D-E**). The lower IC50 values in
235 the case of GIV KO cell lines for all 3 drugs (**Fig 2C**) imply that GIV is required for surviving cytotoxic lesions
236 induced by the most commonly used cytotoxic drugs.

237 Because cell cycle is a key determinant of the choice of repair pathway, next, we asked if GIV may impact
238 one or more of the three checkpoints (G1/S, S phase, and G2/M) where cell cycle may be arrested in response
239 to DNA damage. We found that Dox-challenged parental cells, as expected for cells with defective p53, escaped
240 the G1/S checkpoint (32), and instead, preferentially showed arrest in S/G2 phase; however, GIV KO cells
241 showed no such S phase arrest and instead arrested in the G2 phase (**Fig 2D; Fig S1F**). Because
242 chromosome duplication occurs during the "S phase" (the phase of DNA synthesis) and this phase surveys DNA
243 for replication errors (33), failure of GIV KO cells to arrest in S phase indicates that this "checkpoint" is impaired
244 (i.e., bypassed). Because irreparable DNA injury leads to the accumulation of mutations, which in turn may
245 induce either apoptosis and necrosis (34), next we analyzed cell death by flow cytometry using a combination of
246 annexin V and propidium iodide (PI) staining. Compared to parental control cells, Dox challenge induced a
247 significantly higher rate of cell death in GIV KO cells (**Fig 2E-F; Fig S1G**), *via* both necrosis (**Fig 2E**) and
248 apoptosis (specifically, late apoptosis; **Fig 2F**).

249 To examine whether higher cell death was related to impaired repair activity and an accumulation of DNA
250 strand breaks in GIV KO cells, genomic DNA was isolated from parental and GIV KO cells, with or without Dox
251 challenge and the levels of strand breaks in the *HPRT* and *POLB* genes were compared using long amplicon
252 quantitative PCR (LA-qPCR) as described previously (35). Strand breaks were measured for both the genes
253 using a Poisson distribution, and the results were expressed as the lesion/10 kb genome (36). A decreased level
254 of the long amplicon PCR product (12.2 kb of the *POLB* or 10.4 kb region of the *HPRT* gene) would reflect a
255 higher level of breaks; however, amplification of a smaller fragment for each gene is expected to be similar for
256 the samples, because of a lower probability of breaks within a shorter fragment. A higher level of DNA lesion
257 frequency was observed per 10 Kb in the genomic DNA of GIV KO cells than in the DNA of parental controls
258 (**Fig 2G-H; Fig S1H**), indicating a role of GIV in DNA repair.

259 Reduced cell survival (**Fig 2C**), cell cycle arrest (**Fig 2D**), higher cell death (**Fig 2E-F**) and the
260 accumulation of cytotoxic lesions (**Fig 2G-H**) in GIV KO cells was also associated with reduced growth in
261 anchorage-dependent colonogenic growth assays (**Fig S1I**).

262 To test if the pro-survival functions of GIV in the setting of cytotoxic lesions is cell-type specific, we
263 compared 2 other cell lines, the MDA-MB-231 breast and DLD-1 colorectal cancer lines (**Fig S2A**). We generated
264 GIV KO MDA-MB-231 cell lines using CRISPR Cas9 (see validation in **Fig S2B-C**) and used the previously
265 validated GIV KO DLD-1 cells (37). We exposed these cells to Doxorubicin. Survival was significantly impaired
266 in all the GIV KO cell lines (**Fig S2D-F**), implying that our findings in HeLa cells may be broadly relevant in
267 diverse cancers.

268 Taken together, these findings demonstrate that GIV is required for DNA repair; in cells without GIV, cell
269 survival is reduced, S phase checkpoint is lost, and DNA repair is impaired, leading to the accumulation of
270 catastrophic amounts of mutations that ultimately triggers cell death (see **Fig 2I**).

271 ***The C-terminus of GIV binds tandem BRCT modules of BRCA1***

272 We next sought to validate the major BioID-predicted interaction of GIV, i.e., BRCA1. To determine if GIV and
273 BRCA1 interact in cells, we carried out coimmunoprecipitation (Co-IP) assays and found that the two full-length
274 endogenous proteins exist in the same immune complexes (**Fig 3A**). BRCA1 features two prominent modules
275 that mediate protein-protein interactions, an N-terminal RING domain, which functions as an E3 ubiquitin ligase
276 (38), and a C-terminal BRCT repeat domain, which functions as phospho-protein binding module (39). Pulldown
277 assays using recombinant GST-tagged BRCA1-NT (RING) or CT (tandem BRCT repeats) proteins immobilized
278 on Glutathione beads and lysates of HEK cells as a source of FLAG-tagged GIV showed that full-length GIV
279 binds BRCT, but not the RING module (**Fig 3B**). We noted that GIV is predicted to also interact with other BRCT-
280 domain containing DDR pathway proteins, e.g., DNA Ligase IV (LIG4) and Mediator Of DNA Damage Checkpoint
281 1 (MDC1) [Human cell map, cell-map.org; a database of BioID proximity map of the HEK293 proteome;
282 accessed on 01/06/2020] and with BARD1 [BioGRID, thebiogrid.org; accessed 09/05/2020]. Pulldown assays
283 with these BRCT modules showed that GIV bound DNA Ligase and BARD1, but not MDC1 (**Fig 3B**), suggesting
284 that while GIV can promiscuously bind multiple DDR pathway proteins that contain the BRCT module, there may
285 be a basis for selectivity within such apparent promiscuity. As a positive control for BRCT-binding protein, we
286 tracked by immunoblotting the binding of BACH1 from the same lysates, which bound BRCA1's tandem BRCT
287 module, as expected (40), and to a lesser extent with DNA Ligase (**Fig 3B**).

288 We next asked if the C-terminus of GIV can directly bind BRCA1; we focused on GIV's C-terminus (GIV-
289 CT) because numerous studies have underscored the importance of GIV-CT as an unstructured and/or
290 intrinsically disordered domain that scaffolds key proteins within major signaling cascades to mediate dynamic
291 pathway crosstalk (41,42). GST pulldown assays using recombinant His-tagged GIV-CT¹⁶⁶⁰⁻¹⁸⁷⁰ and various
292 GST-DDR pathway proteins showed that GIV's CT is sufficient to bind the C-terminal tandem BRCT domain of
293

BRCA1 (**Fig 3C**). Because we used purified recombinant proteins in this assay, we conclude the GIV•BRCA1 interaction observed in cells is direct. Using lysates from multiple different cell types as source of GIV (Hs578T, **Fig 3D**; Cos7 and HeLa; **Fig S3A-B**) we further confirmed that endogenous full-length GIV binds the C-terminal tandem BRCT domain of BRCA1 (but not its RING domain) and weakly with BARD1.

Domain-mapping efforts, using various fragments of GIV-CT (aa 1623-1870, 1660-1870, and 1790-1870; **Fig. 3E**) helped narrow the region within GIV that binds BRCA1. The longer GIV-CT fragments bound, but the shortest fragment (1790-1870) did not (**Fig. 3E-F**), indicating that the sequence of GIV that lies between aa 1660-1790 could be the key determinant of binding. A sequence alignment of this region on GIV against known interactors of BRCA1's tandem BRCT repeats revealed the presence of a canonical BRCT-binding phosphopeptide sequence of the consensus "phosphoserine (pSer/pS)-x-x-Phenylalanine (Phe; F)" (**Fig 3G**). The structural basis for such binding has been resolved (43). This newly identified putative BRCT-binding motif in GIV had three notable features: First, this motif (¹⁷¹⁶SSDF¹⁷¹⁹) is distinct from and farther downstream of GIV's Gai-modulatory motif (31 aa ~1670-1690) (**Fig S4A**), suggesting that they may be functionally independent. Second, the SxxF motif is evolutionarily conserved in higher vertebrates (birds and mammals) (**Fig S4A**), suggesting that GIV could be a part of the complex regulatory capacities that evolved later (44). Third, multiple independent studies have reported that the Ser in ¹⁷¹⁶SSDF¹⁷¹⁹ is phosphorylated (**Fig S4B**), suggesting that GIV•BRCA1 complexes may be subject to phosphomodulation. Site-directed mutagenesis that destroys the consensus motif (by replacing Phe with Ala; F1719A) resulted in a loss of binding between GIV-CT and BRCA1 (**Fig 3H**), thereby confirming that the putative BRCT-binding motif is functional and implicating it in the GIV•BRCA1 interaction. The independent nature of the BRCA1-binding and Gai-modulatory motif was confirmed in pulldown assays with full-length WT and mutant GIV proteins (**Fig 3I-J**); the BRCA1 binding-deficient F1719A mutant protein selectively lost binding to GST-BRCA1, but not GST-Gai3, and the well-characterized G-protein binding-deficient F1685A mutant protein (20,21) selectively lost binding to GST-Gai3, but not GST-BRCA1.

Collectively, these findings demonstrate that GIV binds BRCA1 via its C-terminally located BRCT-binding motif. This motif is sensitive to disruption *via* a single point mutation but specific enough that such mutation does not alter GIV's ability to bind Gai-proteins.

GIV binds BRCA1 in both phospho-dependent and -independent modes via the same motif

We next asked how GIV binds BRCA1(BRCT). BRCT modules are known to bind ligands *via* two modes—(i) canonical, phospho-dependent (e.g., BACH1, CtIP, Abraxas) and (ii) non-canonical, phospho-independent (e.g., p53) (45); while the structural basis for the former has been resolved (43), the latter remains unclear. Because bacterially expressed His-GIV-CT directly binds the tandem BRCA1-BRCT (**Fig 3C**), the GIV•BRCA1 (BRCT) interaction appears phospho-independent. As positive controls for canonical phospho-dependent binding, we used BACH1 and CtIP, two *bona fide* binding partners of BRCA1-BRCT module. Recombinant His-GIV-CT did not impact the canonical mode of binding of either BACH1 (**Fig 4A**) or CtIP (**Fig 4B**) to BRCA1-BRCT,

329 suggesting that unphosphorylated GIV binds BRCA1 at a site that is distinct from the interdomain cleft where
330 BACH1 or CtIP are known to occupy (43). Furthermore, binding of GIV to the tandem BRCT was enhanced ~3-
331 5-fold in the presence of the most frequently occurring mutation in BRCA1, M1775R (**Fig 4C**); this mutation is
332 known to abrogate canonical mode of phosphopeptide binding by destroying a hydrophobic pocket that otherwise
333 accommodates the Phe in the pSxxF consensus (see **Fig S5A**) (46). The unexpected increase in binding to the
334 BRCA1-M1775R mutant was also observed in the case of p53, which is another phospho-independent
335 BRCA1(BRCT)-interacting partner (47) (**Fig 4D**). The expected disruptive effect of this mutation could, however,
336 be confirmed in the case of both BACH1 (**Fig S5B**) and CtIP (**Fig S5C**). These findings demonstrate that GIV
337 binds BRCA1 *via* a non-canonical phospho-independent mechanism that is distinct from CtIP and BACH1.

338 Because ~10 high-throughput (HTP) studies have confirmed that Ser¹⁷¹⁶ within the BRCA1-binding motif
339 of GIV is phosphorylated (**Fig S5C**), presumably by one of the many DDR and cell-cycle regulatory kinases (**Fig**
340 **S5D**), we asked if the GIV•BRCA1 interaction is phosphomodulated. Phosphomimic (Ser¹⁷¹⁶→Asp; S1716D) and
341 non-phosphorylatable (Ser¹⁷¹⁶→Ala; S1716A) mutants of GST-GIV-CT were generated, rationalized based on
342 systematic peptide screening studies demonstrating that Glu/Asp-x-x-Phe peptides bind BRCT modules with
343 ~10-fold higher affinity (48). Binding of BRCA1 was accentuated with GIV-S1716D mutant but restored to levels
344 similar to WT in the case of GIV-S1716A mutant (**Fig 4E**), indicating that the GIV•BRCA1 interaction may be
345 phosphoenhanced and that the -OH group in Ser (which is absent in Ala; A) is not essential for the interaction.
346 The phosphate group in the consensus pSxxF mediates polar interactions with S1655/G1656 in β1 and K1702
347 in α2 of BRCA1 (43), and a K1702M mutant has previously been shown to impair phospho-dependent canonical
348 mode of binding (44). We found that the observed phosphoenhanced GIV•BRCA1 in **Fig 4E** is virtually abrogated
349 in the case of BRCA1-K1702M (**Fig 4F**), indicating that upon phosphorylation at S1716, GIV may bind BRCA1
350 in a phospho-dependent canonical mode. Finally, in pulldown assays with the BRCA1-M1775R mutant, binding
351 was inhibited to the phosphomimic GIV-S1716D mutant, but not to GIV-WT (**Fig 4G**), likely *via* the obliteration
352 of the binding pocket for the F1719, as has been reported in the canonical binding mode (46). That the F1719 is
353 also important for phospho-dependent binding was also confirmed; the addition of F1719A mutation to S1716D
354 mutation disrupted binding to BRCA1 (**Fig 4H**), indicating that the same BRCA1-binding motif participates in both
355 modes of binding. Homology models of GIV•BRCA1 co-complexes (**Fig 4I; top**), built using the solved structure
356 of canonical BACH1•BRCA1 co-complex (PDB:1T29) as template further confirmed that phospho-dependent
357 canonical mode of binding and disrupted binding when M1775 is mutated to R (**Fig 4I; bottom**) is compatible
358 with the observed biochemical studies.

359 Taken together, these findings support the conclusion that GIV binds BRCA1 in two different modes: a
360 non-canonical phospho-independent mode, the structural basis for which remains unknown (**Fig 4J; left**), and a
361 canonical phospho-dependent mode (**Fig 4J; right**). Both modes of binding occur *via* the same motif in GIV.

362
363 ***Both GIV•BRCA1 and GIV•Gai interactions are required for DNA repair***

To dissect the role of the GIV•BRCA1 interaction, we rescued GIV KO HeLa cell lines with either GIV-WT or single-point specific mutants of GIV that either cannot bind BRCA1 (F1719A) or cannot bind/activate Gai-proteins (F1685A) and used them in the same phenotypic assays as before (**Fig 5A**). First, we confirmed by immunoblotting that the G418-selected clones stably express physiologic amounts of GIV-WT/mutants at levels similar to endogenous (**Fig 5B**). When challenged with Dox, cisplatin, or etoposide, survival, as determined using a MTT assay was significantly reduced in the cells expressing either mutant compared to GIV-WT (**Fig 5C; Fig S6A-C**). The lower IC₅₀ values in the case of GIV mutant cell lines for all 3 drugs (**Fig 5C**) imply that both functions of GIV, i.e., BRCA1-binding and G protein-binding/activating, are required for surviving cytotoxic lesions induced by commonly used cytotoxic drugs. Lower survival was associated with G2/M phase arrest in both mutant lines (**Fig 5D; S6A**). The S phase checkpoint, however, was intact in cells expressing GIV-WT and GIV-F1685A mutant, but not in GIV-F1719A mutant (**Fig 5D**), indicating that disruption of the GIV•BRCA1 interaction blocks the S phase checkpoint. Flow cytometry studies showed that cell death, both necrosis (**Fig 5E, S6B**) and apoptosis (late apoptosis; LAC; **Fig 5F, S6B**), was significantly increased in both mutant-expressing lines compared to GIV-WT. The extent of death was higher in GIV-F1719A mutant lines, indicating that disruption of the GIV•BRCA1 interaction is catastrophic. Consistently, the burden of mutations was increased in both mutant lines, but to a higher degree in GIV-F1719A mutant lines (**Fig 5G-H; S6C**).

Taken together, these results demonstrate that both functions of GIV (BRCA1-binding and Gai binding and activation) are important for GIV's role in mounting a DDR. The use of GIV KO cell lines rescued with WT or specific binding-deficient mutants further pinpointed the role of each function in the process (**Fig 5I**; summarized in **Table 1**). The GIV•BRCA1 interaction was required for S phase checkpoint arrest, cell survival, and DNA repair. However, GIV's Gai-modulatory function was somehow important for cell survival and the efficiency of DNA repair.

GIV inhibits HR and favors NHEJ

We next asked how GIV's ability to bind BRCA1 or activate Gai might impact the choice of the pathway for DNA repair. While γ H2AX is responsible for the recruitment of many DNA maintenance and repair proteins to the damaged sites, including 53BP1 and RAD51 (49), the preferential accumulation of 53BP1 indicates NHEJ, whereas the preferential accumulation of Rad51 indicates HR (12) (**Fig 6A**). BRCA1 favorably activates Rad51-mediated HR repair and actively inhibits 53BP1-mediated NHEJ repair (50). We found that nuclear accumulation of 53BP1, as determined by confocal microscopy, was far greater in parental HeLa cells compared to GIV KO cells (**Fig 6B; left; 6C**). By contrast, nuclear accumulation of Rad51 was much more pronounced in GIV KO compared to parental cells (**Fig 6B; right; 6C'**). These findings indicate that NHEJ is the preferred choice for repair in cells with GIV, but HR is favored in the absence of GIV. This preference of HR over NHEJ in GIV KO cells was reversed in KO cells rescued with GIV-WT but could not be rescued by mutant GIV proteins that could not bind BRCA1 or modulate Gai proteins (**Fig 6D; 6E-E'**). DSBs were increased in GIV KO cells and in cells

expressing either of the GIV mutants, as determined by γ H2AX staining; this is consistent with the prior long amplicon PCR studies assessing the burden of mutations (**Fig 2G-H, 5G-H**).

That GIV is required for NHEJ was further confirmed by live cell imaging using parental and GIV KO HeLa (**Fig 6F-H**) and MDA-MB-231 cells (**Fig S7A-B**) stably expressing a fluorescent reporter of endogenous DSBs, a construct comprised of a truncated segment of p53BP1 fused to mApple (51) (see *Methods for details*). Compared to the parental cells, the fold change in bright foci/cell was significantly decreased in GIV-depleted HeLa and MDA-MB-231 cells regardless of the drugs, duration and concentrations tested.

Taken together, these findings indicate that GIV and its BRCA1-binding and Gai-modulatory functional modules are required for dictating the choice of DDR; when GIV is present and its two functional modules are intact, NHEJ is preferred over HR. It is also noteworthy that the mutational burden is increased despite the DNA damage-induced accumulation of nuclear Rad51, which suggests that HR is initiated successfully, but may not be as effective as NHEJ. The latter offers an ideal balance of flexibility and accuracy in the setting of widespread DSBs with diverse end structures (15).

GIV translocates to the nucleus after DNA damage, inhibits colocalization of BRCA1 with DSBs

Because BRCA1 is a nucleocytoplasmic shuttling protein (52) and it is nuclear BRCA1 that augments DNA repair (53) and cell-cycle checkpoints (54), we asked if suppressed HR in cells with GIV, or those with functionally intact modules in GIV stemmed from mis-localization of BRCA1. We determined the localization of GIV and BRCA1 by confocal immunofluorescence and found that Dox challenge was associated with nuclear localization of GIV (see Parental cells; **Fig 6F, top**). Compared to parental control cells, nuclear localization of BRCA1 was more prominent in GIV KO cells, where it colocalized with γ H2AX (see Parental cells; **Fig 6F, bottom**), indicating that nuclear localization of BRCA1 to sites of DSBs may be suppressed by GIV.

To discern which functional module of GIV may be important for nuclear localization of GIV and/or suppression of nuclear localization of BRCA1, we carried out similar assays in stable cell lines expressing GIV-WT or mutant. DNA damage dependent shuttling of GIV to the nucleus was observed in the case of GIV-WT and GIV-F1719A, but not GIV-F1685A (see **Fig 6G, top**), indicating that GIV's ability to shuttle into the nucleus after DNA damage does not depend on its interaction with BRCA1, but requires a functionally intact Gai-modulatory function. We observed prominent nuclear localization of BRCA1 only in the GIV-F1719A mutant line, where it colocalized with γ H2AX (see **Fig 6G, bottom**). Colocalization coefficient of BRCA1 with γ H2AX across all cell lines (**Fig 6H; S7C**) showed that colocalization was greatest in the absence of GIV (GIV KO cells) or when the GIV•BRCA1 interaction is impaired (F1719A), indicating that the GIV•BRCA1 interaction is required for the observed inhibitory effect of GIV on nuclear localization of BRCA1.

Taken together, these findings demonstrate that GIV, like BRCA1, is a nucleocytoplasmic shuttling protein; shuttling is independent of its BRCA1-binding function but depends on its Gai-modulatory function. The GIV•BRCA1 interaction appears to be primarily responsible for sequestering BRCA1 away from DSBs.

434 Localization of BRCA1 at sites of DSBs is not only impaired in the case of GIV-WT expressing cells, in which
435 GIV shuttles into the nucleus upon DNA damage, but also impaired in GIV-F1685A mutant cells (**Fig 6H; S7D**),
436 in which GIV fails to localize to the nucleus. This indicates that the inhibitory GIV•BRCA1 interaction may occur
437 in the nucleus as well as in the cytoplasm, and is in keeping with our BioID studies revealing BRCA1 as a
438 candidate interactor of GIV in both nuclear and cytosolic compartments (**Fig 1C**).

439 ***GIV's Gai-modulatory function activates Akt, BRCA1-binding function triggers S-phase checkpoint***

440 Because the choice of DNA damage repair pathway is finetuned by a network of kinases (e.g., ATM, ATR, Akt,
441 etc.) and the signaling cascades they initiate (55,56), we asked how GIV and its functional modules may impact
442 these pathways. More specifically, we focused on two key readouts rationalized by our observations: (i) Akt
443 phosphorylation, because GIV is a *bona fide* enhancer of Akt phosphorylation (57,58) and does so via its Gai-
444 modulatory function (20), and because this pathway is known to impact the choice of repair [reviewed in (56)];
445 (ii) Phosphorylation of the cohesion protein, Structural Maintenance of Chromosome-1 (pSer-957 SMC1) (59), a
446 readout of S-phase checkpoint, because this checkpoint was impaired in GIV KO cells (**Fig 2D**). We found that
447 the depletion of GIV significantly reduced phosphorylation of both readouts (**Fig 7A-C**), indicating that GIV is
448 required for the phosphoactivation of both the Akt and the ATM→pSMC1 axes. Similar studies on HeLa cell lines
449 stably expressing GIV-WT or mutants showed that Akt phosphorylation was impaired in both GIV-F1685A and
450 GIV-F1719A mutants (**Fig 7D, 7E**), albeit more significantly impaired in the latter, but phosphoSMC1 was
451 specifically impaired in cells expressing the GIV-F1719A mutant (**Fig 7D, 7F**). These findings show that the
452 BRCA1-binding function of GIV is critical for initiation of Akt signaling upon DNA damage, as well as for the
453 activation of the ATM→pSMC1 pathway for S-phase checkpoint signaling. The Gai-modulatory function of GIV,
454 however, was specifically responsible for enhancing Akt signals after DNA damage.

455 We asked if the previously delineated Gi → 'free' Gbg release → Class 1 PI3K signaling axis triggered
456 by GIV's Gai-modulatory function may be essential (20). To this end, we first assessed the extent of activation
457 of Gai in cells after DNA damage by using a conformation-sensing antibody that specifically recognizes GTP-
458 bound (active) conformation of Gai1-3 (**Fig 7G; top**) (60), and more importantly, recognizes GIV-dependent G
459 protein activation in cells (42). We found that DNA damage was associated with activation of Gai in parental
460 cells, but that such activation was virtually lost in GIV KO cells (**Fig 7G; bottom**). To dissect if Akt activation is
461 mediated *via* the 'free' Gbg→Class 1 PI3K signaling axis, we used the commonly used small molecule Gbg
462 inhibitor, Gallein (**Fig 7H; top**), and its inactive isomer, Fluorescein (negative control) (61). We found that
463 Gallein, but not Fluorescein inhibited DNA damage-induced Akt phosphorylation in parental control cells,
464 reducing it to the levels observed in GIV KO cells (**Fig 7H; bottom**). These findings indicate that Akt signaling
465 induced after DNA damage, occurs in part *via* GIV-dependent Gi activation.

466 Taken together, our findings support the following working model for how GIV dictates the choice of repair
467 pathway after DNA damage, favoring NHEJ over HR (**Fig 7I**). Using a set of single points mutants and chemical
468

469 inhibitors of G protein signaling, we charted the mechanisms that allow GIV to accomplish such a goal *via* two
470 parallel pathways (see **Fig 7J**). One pathway is mediated by GIV's ability to bind and sequester BRCA1 in the
471 cytoplasmic pool, and thereby reduce its ability to localize to DSBs, suppress HR, and activate S phase
472 checkpoint cascades. Another is GIV's ability to bind and activate Gi and enhance Akt signaling, which is known
473 to further skew the choice of repair pathway towards NHEJ, while actively suppressing HR.

474

475

476 Conclusions

477 Cellular decision-making in response to any stressful insult, is mediated by a web of spatiotemporally segregated
478 events within the intracellular signaling networks, often requiring crosstalk between unlikely pathways. The major
479 discovery we report here is such an unexpected crosstalk that is orchestrated *via* a versatile multi-modular signal
480 transducer, GIV/Girdin. There are three notable takeaways from this study.

481 First, this work ushers a new player in DNA repair. Although GIV entered the field of cancer biology more
482 than a decade ago, and quickly came to be known as a pro-oncogenic protein that coupled G protein signaling
483 with unlikely pathways [reviewed in (24)], its role inside the nucleus remained unknown. Although predicted to
484 have nuclear localization signals (NLS; **Table 2**), how GIV shuttles into the nucleus remains unresolved.
485 Regardless, what emerged using specific single-point mutants is that GIV inhibits HR by sequestering BRCA1,
486 suppressing its localization to DSBs. Although how GIV binds BRCA1 was studied at greater depth (expanded
487 below), how exactly GIV may inhibit the shuttling/localization of BRCA1 remains unresolved. Because nuclear
488 import of BRCA1 and its retention requires BARD1 (62), whereas nuclear export requires p53 (63), GIV may
489 either inhibit the BARD1•BRCA1 interplay or augment the actions of p53.

490 Second, one of the most unexpected observations was that GIV uses the same short linear motif (SLIM)
491 located within its C-terminus to bind the C-terminal tandem-BRCT modules of BRCA1 in both canonical
492 (phospho-dependent) and non-canonical (phospho-independent) modes. Although both modes of BRCT-binding
493 has been recognized in other instances (45), the versatility of dual-mode binding *via* the same motif is
494 unprecedented. Given this degree of versatility of the BRCT-binding SLIM in GIV, and the additional BRCT
495 interactors we found here (to DNA Lig IV and BARD1), it is more likely than not that this SLIM binds other players
496 within the DDR pathways. Who binds, and who does not may be dictated by the residues flanking the SLIM, as
497 shown in other instances (64). These findings are in keeping with the fact that GIV-CT is an intrinsically
498 disordered protein (IDP) (41,65) comprised of distinct SLIMs, of which the BRCT-binding motif described here is
499 an example (see **Fig S3A**). SLIMs enable GIV to couple G protein signaling to a myriad of molecular sensors, of
500 both the outside of the cell (i.e., receptors; [reviewed in (66)]) or its interior (67). Because IDPs that fold/unfold
501 on demand expose/hide SLIMs, which in turn imparts plasticity to protein-protein interaction networks during
502 signal transduction (68), GIV may do something similar in couple G protein signaling to DDR. By scaffolding G
503 proteins to BRCT-modules in BRCA1 (and presumably other DDR proteins) GIV may serve as a point of
504 convergence for coordinating signaling events and generating pathway crosstalk upon DNA damage.

505 Third, this work provides a direct mechanistic link between DDR and trimeric G proteins; the latter is one
506 of the major pervasive signaling hubs in eukaryotic cells that was notably absent from the field of DNA repair.
507 Although multiple peripheral components within the GPCR/G-protein signaling system has been found to
508 indirectly influence DNA damage and/or repair (23), who/what might activate G proteins on endomembranes
509 was unknown. We demonstrated that trimeric Gi proteins are activated upon DNA damage, and that such
510 activation requires GIV's Gai-modulatory motif. That the GIV→Gai pathway activates Akt signaling helps explain

511 the hitherto elusive origin of Akt signaling during DDR (56). That GIV favors NHEJ over HR and activates Akt
512 signaling during DDR is in keeping with the previously described role of Akt signaling in dictating the choice of
513 repair pathway (56).

514 In closing, damage to the genome can have catastrophic consequences, including cytotoxicity,
515 accelerated aging, and predisposition to cancers. Our findings, which revealed a hitherto unknown link between
516 a major hub in DNA repair (i.e., BRCA1) and a signaling hub of paramount importance in just about all aspects
517 of modern medicine (trimeric G proteins) opens new avenues for development of novel therapeutic strategies.

518 **Materials and Methods**

519 All methods are detailed in *SI Appendix*, and briefly mentioned here.

520
521 *Statistical Analysis and Replicates*

522 All experiments were repeated at least three times, and results were presented either as average \pm SEM.

523 Statistical significance was assessed using one-way analysis of variance (ANOVA) including a Tukey's test for
524 multiple comparisons. * $p < 0.05$, ** $p < 0.01$, *** $p < 0.001$, **** $p < 0.0001$.

References Cited

1. Tubbs, A. and Nussenzweig, A. (2017) Endogenous DNA damage as a source of genomic instability in cancer. *Cell*, **168**, 644-656.
2. Jackson, S.P. and Bartek, J. (2009) The DNA-damage response in human biology and disease. *Nature*, **461**, 1071-1078.
3. Giglia-Mari, G., Zotter, A. and Vermeulen, W. (2011) DNA damage response. *Cold Spring Harbor perspectives in biology*, **3**, a000745.
4. Blackford, A.N. and Jackson, S.P. (2017) ATM, ATR, and DNA-PK: the trinity at the heart of the DNA damage response. *Molecular cell*, **66**, 801-817.
5. van den Bosch, M., Bree, R.T. and Lowndes, N.F. (2003) The MRN complex: coordinating and mediating the response to broken chromosomes. *EMBO reports*, **4**, 844-849.
6. Burma, S., Chen, B.P., Murphy, M., Kurimasa, A. and Chen, D.J. (2001) ATM phosphorylates histone H2AX in response to DNA double-strand breaks. *Journal of Biological Chemistry*, **276**, 42462-42467.
7. Van Attikum, H. and Gasser, S.M. (2009) Crosstalk between histone modifications during the DNA damage response. *Trends in cell biology*, **19**, 207-217.
8. Polo, S.E. and Jackson, S.P. (2011) Dynamics of DNA damage response proteins at DNA breaks: a focus on protein modifications. *Genes & development*, **25**, 409-433.
9. Shi, L. and Oberdoerffer, P. (2012) Chromatin dynamics in DNA double-strand break repair. *Biochimica Et Biophysica Acta (BBA)-Gene Regulatory Mechanisms*, **1819**, 811-819.
10. Bouwman, B.A. and Crosetto, N. (2018) Endogenous DNA double-strand breaks during DNA transactions: emerging insights and methods for genome-wide profiling. *Genes*, **9**, 632.
11. Allen, C., Halbrook, J. and Nickoloff, J.A. (2003) Interactive competition between homologous recombination and non-homologous end joining 11NIH grant CA77693 to JAN. *Molecular Cancer Research*, **1**, 913-920.
12. Brandsma, I. and van Gent, D.C. (2012) Pathway choice in DNA double strand break repair: observations of a balancing act. *Genome integrity*, **3**, 9.
13. Li, X. and Heyer, W.-D. (2008) Homologous recombination in DNA repair and DNA damage tolerance. *Cell research*, **18**, 99-113.
14. Chakraborty, A., Tapryal, N., Venkova, T., Mitra, J., Vasquez, V., Sarker, A.H., Duarte-Silva, S., Huai, W., Ashizawa, T. and Ghosh, G. (2020) Deficiency in classical nonhomologous end-joining-mediated repair of transcribed genes is linked to SCA3 pathogenesis. *Proceedings of the National Academy of Sciences*, **117**, 8154-8165.
15. Waters, C.A., Strande, N.T., Wyatt, D.W., Pryor, J.M. and Ramsden, D.A. (2014) Nonhomologous end joining: a good solution for bad ends. *DNA repair*, **17**, 39-51.

- 560 16. Vítor, A.C., Huertas, P., Legube, G. and de Almeida, S.F. (2020) Studying DNA double-strand break
561 repair: an ever-growing toolbox. *Frontiers in molecular biosciences*, **7**, 24.
- 562 17. Miki, Y., Swensen, J., Shattuck-Eidens, D., Futreal, P.A., Harshman, K., Tavtigian, S., Liu, Q., Cochran,
563 C., Bennett, L.M. and Ding, W. (1994) A strong candidate for the breast and ovarian cancer
564 susceptibility gene BRCA1. *Science*, **266**, 66-71.
- 565 18. Ceccaldi, R., Rondinelli, B. and D'Andrea, A.D. (2016) Repair pathway choices and consequences at
566 the double-strand break. *Trends in cell biology*, **26**, 52-64.
- 567 19. Daley, J.M. and Sung, P. (2014) 53BP1, BRCA1, and the choice between recombination and end
568 joining at DNA double-strand breaks. *Molecular and cellular biology*, **34**, 1380-1388.
- 569 20. Garcia-Marcos, M., Ghosh, P. and Farquhar, M.G. (2009) GIV is a nonreceptor GEF for Gai with a
570 unique motif that regulates Akt signaling. *Proceedings of the National Academy of Sciences*, **106**, 3178-
571 3183.
- 572 21. Kalogriopoulos, N.A., Rees, S.D., Ngo, T., Kopcho, N.J., Ilatovskiy, A.V., Sun, N., Komives, E.A.,
573 Chang, G., Ghosh, P. and Kufareva, I. (2019) Structural basis for GPCR-independent activation of
574 heterotrimeric Gi proteins. *Proceedings of the National Academy of Sciences*, **116**, 16394-16403.
- 575 22. Santos, R., Ursu, O., Gaulton, A., Bento, A.P., Donadi, R.S., Bologa, C.G., Karlsson, A., Al-Lazikani, B.,
576 Hersey, A. and Oprea, T.I. (2017) A comprehensive map of molecular drug targets. *Nature reviews*
577 *Drug discovery*, **16**, 19-34.
- 578 23. Leysen, H., Van Gastel, J., Hendrickx, J.O., Santos-Otte, P., Martin, B. and Maudsley, S. (2018) G
579 protein-coupled receptor systems as crucial regulators of DNA damage response processes.
580 *International journal of molecular sciences*, **19**, 2919.
- 581 24. Aznar, N., Kalogriopoulos, N., Midde, K.K. and Ghosh, P. (2016) Heterotrimeric G protein signaling via
582 GIV/Girdin: Breaking the rules of engagement, space, and time. *Bioessays*, **38**, 379-393.
- 583 25. Matsushita, E., Asai, N., Enomoto, A., Kawamoto, Y., Kato, T., Mii, S., Maeda, K., Shibata, R., Hattori,
584 S. and Hagikura, M. (2011) Protective role of Gipié, a Girdin family protein, in endoplasmic reticulum
585 stress responses in endothelial cells. *Molecular biology of the cell*, **22**, 736-747.
- 586 26. Ghosh, P. (2015) Heterotrimeric G proteins as emerging targets for network based therapy in cancer:
587 End of a long futile campaign striking heads of a Hydra. *Aging (Albany NY)*, **7**, 469.
- 588 27. Ghosh, P., Garcia-Marcos, M., Bornheimer, S.J. and Farquhar, M.G. (2008) Activation of Gai3 triggers
589 cell migration via regulation of GIV. *The Journal of cell biology*, **182**, 381-393.
- 590 28. Yu, X.-P., Wu, Y.-M., Liu, Y., Tian, M., Wang, J.-D., Ding, K.-K., Ma, T. and Zhou, P.-K. (2017) IER5 is
591 involved in DNA double-strand breaks repair in association with PAPR1 in Hela cells. *International*
592 *Journal of Medical Sciences*, **14**, 1292.
- 593 29. Leroy, B., Girard, L., Hollestelle, A., Minna, J.D., Gazdar, A.F. and Soussi, T. (2014) Analysis of TP 53
594 Mutation Status in Human Cancer Cell Lines: A Reassessment. *Human mutation*, **35**, 756-765.

- 595 30. MATLASHEWSKI, G., BANKS, L., PIM, D. and CRAWFORD, L. (1986) Analysis of human p53 proteins
596 and mRNA levels in normal and transformed cells. *European journal of biochemistry*, **154**, 665-672.
- 597 31. Potter, A.J., Gollahon, K.A., Palanca, B.J., Harbert, M.J., Choi, Y.M., Moskovitz, A.H., Potter, J.D. and
598 Rabinovitch, P.S. (2002) Flow cytometric analysis of the cell cycle phase specificity of DNA damage
599 induced by radiation, hydrogen peroxide and doxorubicin. *Carcinogenesis*, **23**, 389-401.
- 600 32. Senturk, E. and Manfredi, J.J. (2013), *p53 Protocols*. Springer, pp. 49-61.
- 601 33. Das-Bradoo, S. and Bielinsky, A. (2010) DNA replication and checkpoint control in S phase. *Nature*, **9**,
602 74-79.
- 603 34. Nowsheen, S. and Yang, E. (2012) The intersection between DNA damage response and cell death
604 pathways. *Experimental oncology*, **34**, 243.
- 605 35. Dey, S., Maiti, A.K., Hegde, M.L., Hegde, P.M., Boldogh, I., Sarkar, P.S., Abdel-Rahman, S.Z., Sarker,
606 A.H., Hang, B. and Xie, J. (2012) Increased risk of lung cancer associated with a functionally impaired
607 polymorphic variant of the human DNA glycosylase NEIL2. *DNA repair*, **11**, 570-578.
- 608 36. Ayala-Torres, S., Chen, Y., Svoboda, T., Rosenblatt, J. and Van Houten, B. (2000) Analysis of gene-
609 specific DNA damage and repair using quantitative polymerase chain reaction. *Methods*, **22**, 135-147.
- 610 37. Ear, J., Abd El-Hafeez, A.A., Roy, S., Ngo, T., Rajapakse, N., Choi, J., Khandelwal, S., Ghassemian,
611 M., McCaffrey, L. and Kufareva, I. (2021) A long isoform of GIV/Girdin contains a PDZ-binding module
612 that regulates localization and G-protein binding. *Journal of Biological Chemistry*, **296**.
- 613 38. Wu, L.C., Wang, Z.W., Tsan, J.T., Spillman, M.A., Phung, A., Xu, X.L., Yang, M.-C.W., Hwang, L.-Y.,
614 Bowcock, A.M. and Baer, R. (1996) Identification of a RING protein that can interact in vivo with the
615 BRCA1 gene product. *Nature genetics*, **14**, 430-440.
- 616 39. Yu, X., Chini, C.C.S., He, M., Mer, G. and Chen, J. (2003) The BRCT domain is a phospho-protein
617 binding domain. *Science*, **302**, 639-642.
- 618 40. Cantor, S.B., Bell, D.W., Ganesan, S., Kass, E.M., Drapkin, R., Grossman, S., Wahrer, D.C., Sgroi,
619 D.C., Lane, W.S. and Haber, D.A. (2001) BACH1, a novel helicase-like protein, interacts directly with
620 BRCA1 and contributes to its DNA repair function. *Cell*, **105**, 149-160.
- 621 41. Lin, C., Ear, J., Midde, K., Lopez-Sanchez, I., Aznar, N., Garcia-Marcos, M., Kufareva, I., Abagyan, R.
622 and Ghosh, P. (2014) Structural basis for activation of trimeric Gi proteins by multiple growth factor
623 receptors via GIV/Girdin. *Molecular biology of the cell*, **25**, 3654-3671.
- 624 42. Ma, G.S., Aznar, N., Kalogiropoulos, N., Midde, K.K., Lopez-Sanchez, I., Sato, E., Dunkel, Y., Gallo,
625 R.L. and Ghosh, P. (2015) Therapeutic effects of cell-permeant peptides that activate G proteins
626 downstream of growth factors. *Proceedings of the National Academy of Sciences*, **112**, E2602-E2610.
- 627 43. Williams, R.S., Lee, M.S., Hau, D.D. and Glover, J.M. (2004) Structural basis of phosphopeptide
628 recognition by the BRCT domain of BRCA1. *Nature structural & molecular biology*, **11**, 519-525.

- 629 44. Dever, S.M., Golding, S.E., Rosenberg, E., Adams, B.R., Idowu, M.O., Quillin, J.M., Valerie, N., Xu, B.,
630 Povirk, L.F. and Valerie, K. (2011) Mutations in the BRCT binding site of BRCA1 result in hyper-
631 recombination. *Aging (Albany NY)*, **3**, 515.
- 632 45. Leung, C.C.Y. and Glover, J.M. (2011) BRCT domains: easy as one, two, three. *Cell cycle*, **10**, 2461-
633 2470.
- 634 46. Williams, R.S. and Glover, J.M. (2003) Structural consequences of a cancer-causing BRCA1-BRCT
635 missense mutation. *Journal of Biological Chemistry*, **278**, 2630-2635.
- 636 47. Jiang, J., Yang, E.S., Jiang, G., Nowsheen, S., Wang, H., Wang, T., Wang, Y., Billheimer, D.,
637 Chakravarthy, A.B. and Brown, M. (2011) p53-dependent BRCA1 nuclear export controls cellular
638 susceptibility to DNA damage. *Cancer research*, **71**, 5546-5557.
- 639 48. White, E.R., Sun, L., Ma, Z., Beckta, J.M., Danzig, B.A., Hacker, D.E., Huie, M., Williams, D.C.,
640 Edwards, R.A. and Valerie, K. (2015) Peptide library approach to uncover phosphomimetic inhibitors of
641 the BRCA1 C-terminal domain. *ACS chemical biology*, **10**, 1198-1208.
- 642 49. Scully, R. and Xie, A. (2013) Double strand break repair functions of histone H2AX. *Mutation
643 Research/Fundamental and Molecular Mechanisms of Mutagenesis*, **750**, 5-14.
- 644 50. Prakash, R., Zhang, Y., Feng, W. and Jasin, M. (2015) Homologous recombination and human health:
645 the roles of BRCA1, BRCA2, and associated proteins. *Cold Spring Harbor perspectives in biology*, **7**,
646 a016600.
- 647 51. Yang, K.S., Kohler, R.H., Landon, M., Giedt, R. and Weissleder, R. (2015) Single cell resolution in vivo
648 imaging of DNA damage following PARP inhibition. *Scientific reports*, **5**, 1-13.
- 649 52. Fabbro, M. and Henderson, B.R. (2003) Regulation of tumor suppressors by nuclear-cytoplasmic
650 shuttling. *Experimental cell research*, **282**, 59-69.
- 651 53. Zhang, J. and Powell, S.N. (2005) The role of the BRCA1 tumor suppressor in DNA double-strand
652 break repair. *Molecular Cancer Research*, **3**, 531-539.
- 653 54. Mullan, P., Quinn, J. and Harkin, D. (2006) The role of BRCA1 in transcriptional regulation and cell
654 cycle control. *Oncogene*, **25**, 5854-5863.
- 655 55. Maréchal, A. and Zou, L. (2013) DNA damage sensing by the ATM and ATR kinases. *Cold Spring
656 Harbor perspectives in biology*, **5**, a012716.
- 657 56. Liu, Q., Turner, K.M., Alfred Yung, W., Chen, K. and Zhang, W. (2014) Role of AKT signaling in DNA
658 repair and clinical response to cancer therapy. *Neuro-oncology*, **16**, 1313-1323.
- 659 57. Enomoto, A., Murakami, H., Asai, N., Morone, N., Watanabe, T., Kawai, K., Murakumo, Y., Usukura, J.,
660 Kaibuchi, K. and Takahashi, M. (2005) Akt/PKB regulates actin organization and cell motility via
661 Girdin/APE. *Developmental cell*, **9**, 389-402.

- 662 58. Anai, M., Shojima, N., Katagiri, H., Ogihara, T., Sakoda, H., Onishi, Y., Ono, H., Fujishiro, M.,
663 Fukushima, Y. and Horike, N. (2005) A novel protein kinase B (PKB)/AKT-binding protein enhances
664 PKB kinase activity and regulates DNA synthesis. *Journal of Biological Chemistry*, **280**, 18525-18535.
- 665 59. Kim, S.-T., Xu, B. and Kastan, M.B. (2002) Involvement of the cohesin protein, Smc1, in Atm-
666 dependent and independent responses to DNA damage. *Genes & development*, **16**, 560-570.
- 667 60. Lane, J.R., Henderson, D., Powney, B., Wise, A., Rees, S., Daniels, D., Plumpton, C., Kinghorn, I. and
668 Milligan, G. (2008) Antibodies that identify only the active conformation of Gi family G protein α
669 subunits. *The FASEB Journal*, **22**, 1924-1932.
- 670 61. Bonacci, T.M., Mathews, J.L., Yuan, C., Lehmann, D.M., Malik, S., Wu, D., Font, J.L., Bidlack, J.M. and
671 Smrcka, A.V. (2006) Differential targeting of G $\beta\gamma$ -subunit signaling with small molecules. *Science*, **312**,
672 443-446.
- 673 62. Fabbro, M., Rodriguez, J.A., Baer, R. and Henderson, B.R. (2002) BARD1 induces BRCA1 intranuclear
674 foci formation by increasing RING-dependent BRCA1 nuclear import and inhibiting BRCA1 nuclear
675 export. *Journal of Biological Chemistry*, **277**, 21315-21324.
- 676 63. Feng, Z., Kachnic, L., Zhang, J., Powell, S.N. and Xia, F. (2004) DNA damage induces p53-dependent
677 BRCA1 nuclear export. *Journal of Biological Chemistry*, **279**, 28574-28584.
- 678 64. Wu, Q., Jubb, H. and Blundell, T.L. (2015) Phosphopeptide interactions with BRCA1 BRCT domains:
679 More than just a motif. *Progress in biophysics and molecular biology*, **117**, 143-148.
- 680 65. Rohena, C., Kalogriopoulos, N., Rajapakse, N., Roy, S., Lopez-Sanchez, I., Ablack, J., Sahoo, D. and
681 Ghosh, P. (2020) GIV• Kindlin interaction is required for Kindlin-Mediated Integrin Recognition and
682 Activation. *iScience*, 101209.
- 683 66. Midde, K.K., Aznar, N., Laederich, M.B., Ma, G.S., Kunkel, M.T., Newton, A.C. and Ghosh, P. (2015)
684 Multimodular biosensors reveal a novel platform for activation of G proteins by growth factor receptors.
685 *Proceedings of the National Academy of Sciences*, **112**, E937-E946.
- 686 67. Garcia-Marcos, M., Ear, J., Farquhar, M.G. and Ghosh, P. (2011) A GDI (AGS3) and a GEF (GIV)
687 regulate autophagy by balancing G protein activity and growth factor signals. *Molecular biology of the*
688 *cell*, **22**, 673-686.
- 689 68. Wright, P.E. and Dyson, H.J. (2015) Intrinsically disordered proteins in cellular signalling and regulation.
690 *Nat Rev Mol Cell Biol*, **16**, 18-29.
- 691
692
693
694
695
696

697 **ACKNOWLEDGEMENTS**

698
699 This work was supported by the National Institute of Health Grants: CA238042 (to P.G and G.D.L), AI141630,
700 CA100768, CA160911 and UG3TR002968 (to P.G.), U01CA210152, R01CA238023, R33CA225549 and
701 R37CA222563 (GDL), HL145477 (to T.K.H.), R50CA221807 (to K.E.L) and DK107585 (S.D). T.K.H was also
702 supported by NS073976 and W81XWH-18-1-0743. A.A.A was supported by an NIH-funded Cancer Therapeutics
703 Training Program (CT2, T32 CA121938). J.E was supported by an NCI/NIH-funded Cancer Biology, Informatics
704 & Omics (CBIO) Training Program (T32 CA067754) and a Postdoctoral Fellowship from the American Cancer
705 Society (PF-18-101-01- CSM). S.R was supported, in part, by the NIH grants (AI118985 and GM117424).

706 707 708 **AUTHOR CONTRIBUTIONS**

709 A. A. A. and P.G designed, executed and analyzed most of the experiments in this work. N.S. carried out all work
710 related to the generation of constructs used in this work. N.S, P.C., and N.R conducted the protein chemistry
711 and biochemical analyses of the protein-protein interactions. A.C. and A.A.A. designed, executed, and analyzed
712 the DNA mutation load assays in consultation with S.D and supervised by T.K.H. J.E designed, executed, and
713 analyzed the BioID studies. S.R. carried out the structural modeling and analyses with supervision from P.G.
714 K.E.L and G.D.L designed, executed, and analyzed the 53BP1 reporter studies in live cells. A. A. A., A.C and
715 S.R wrote methods. A.A.A and P.G conceived the project, wrote and edited the manuscript.

716 717 **Corresponding author**

718 Correspondence to Pradipta Ghosh

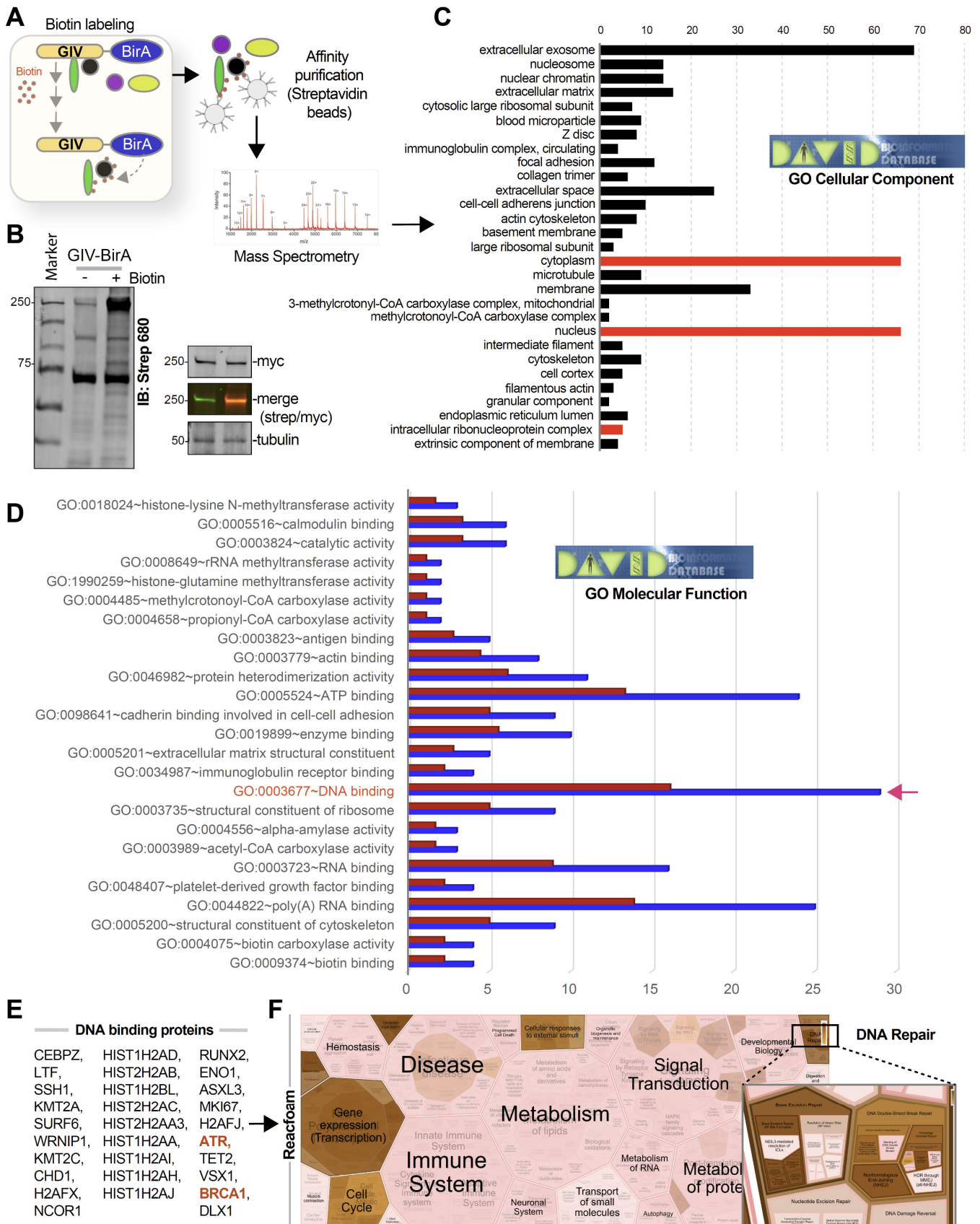
719 720 **Competing interests**

721 All authors declare no competing interests.

722
723
724
725
726

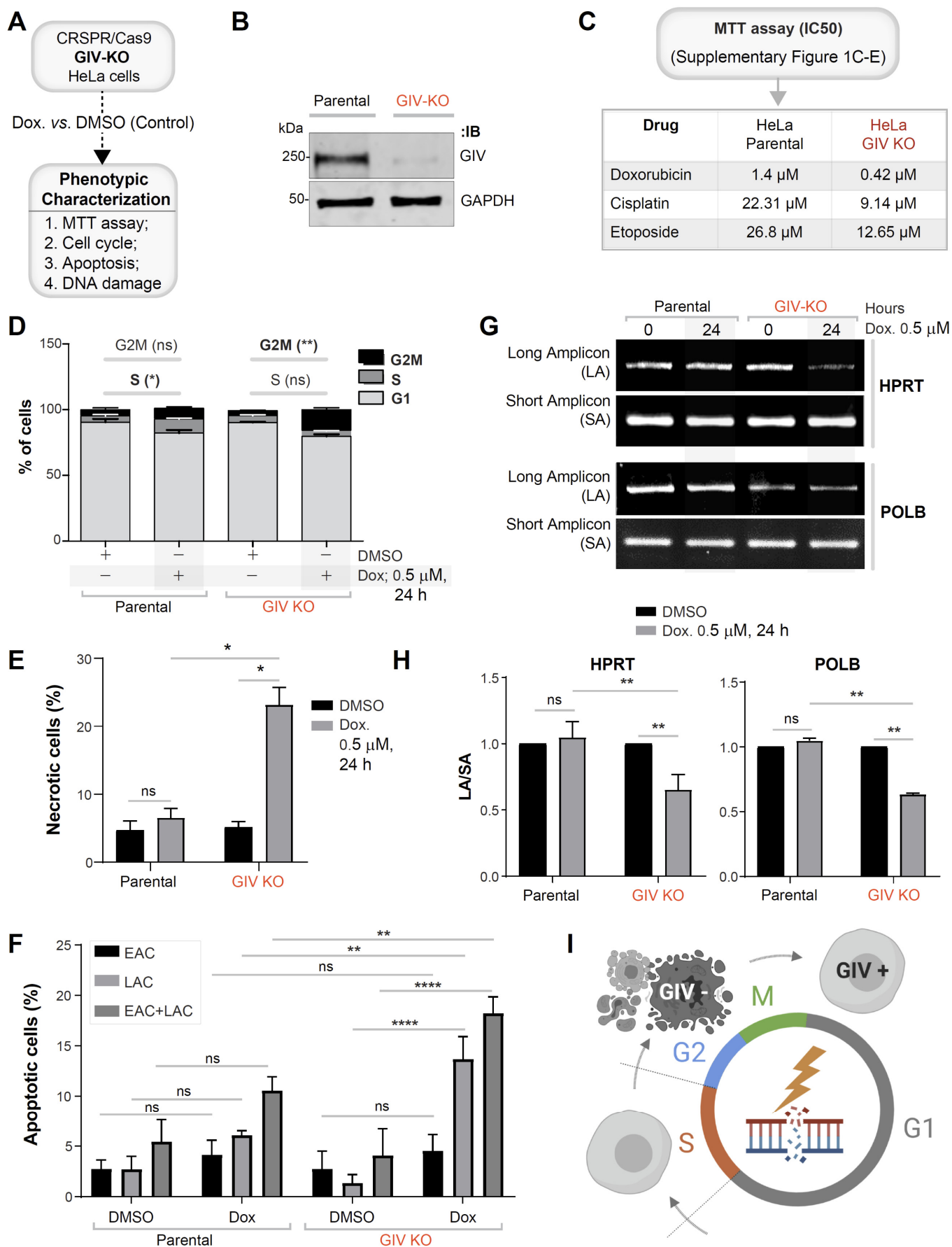
727

Figures and legends

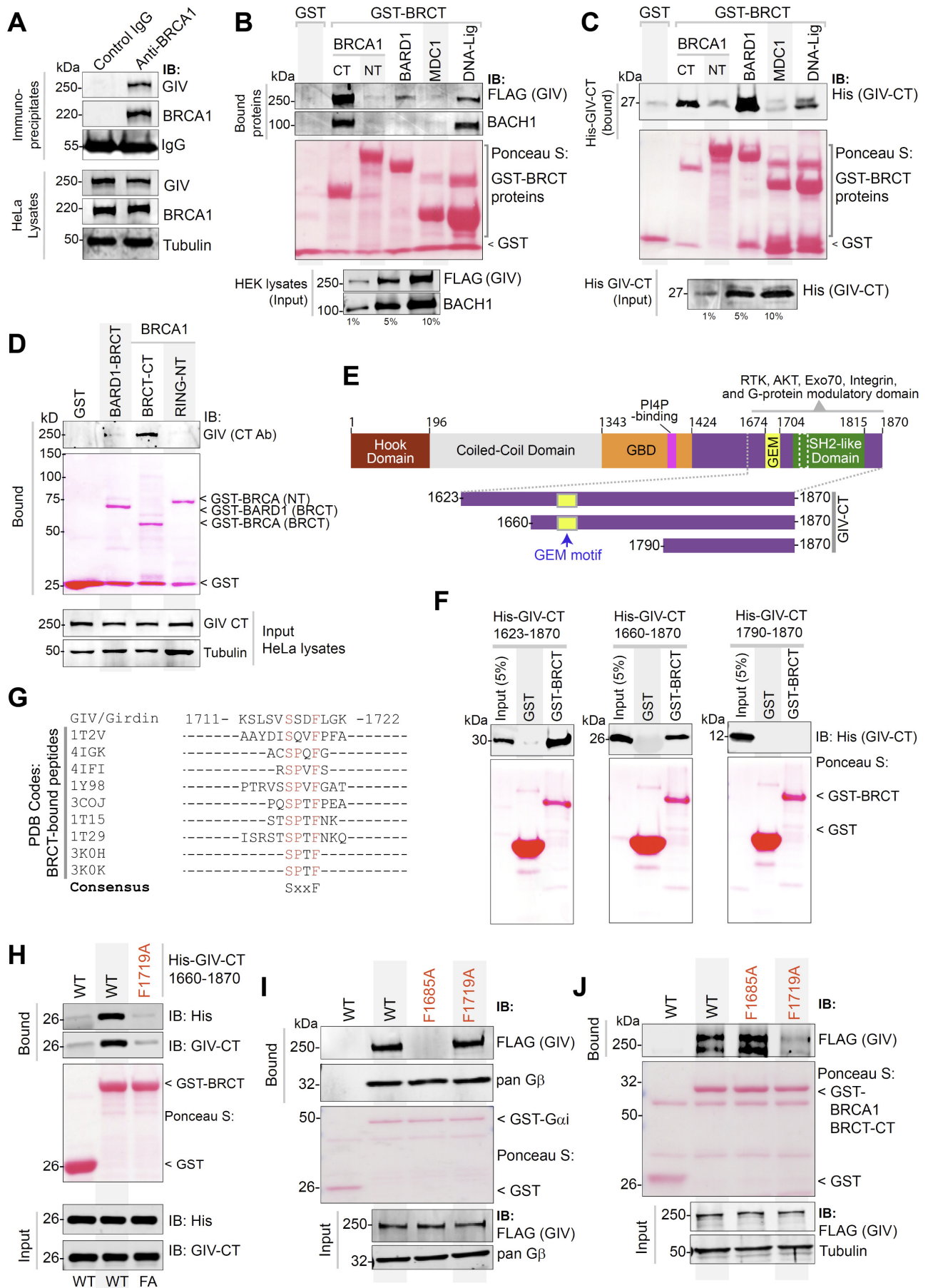


728 **Figure 1. Proteomic studies suggest an intranuclear role of GIV/Girdin in DNA damage repair response.**

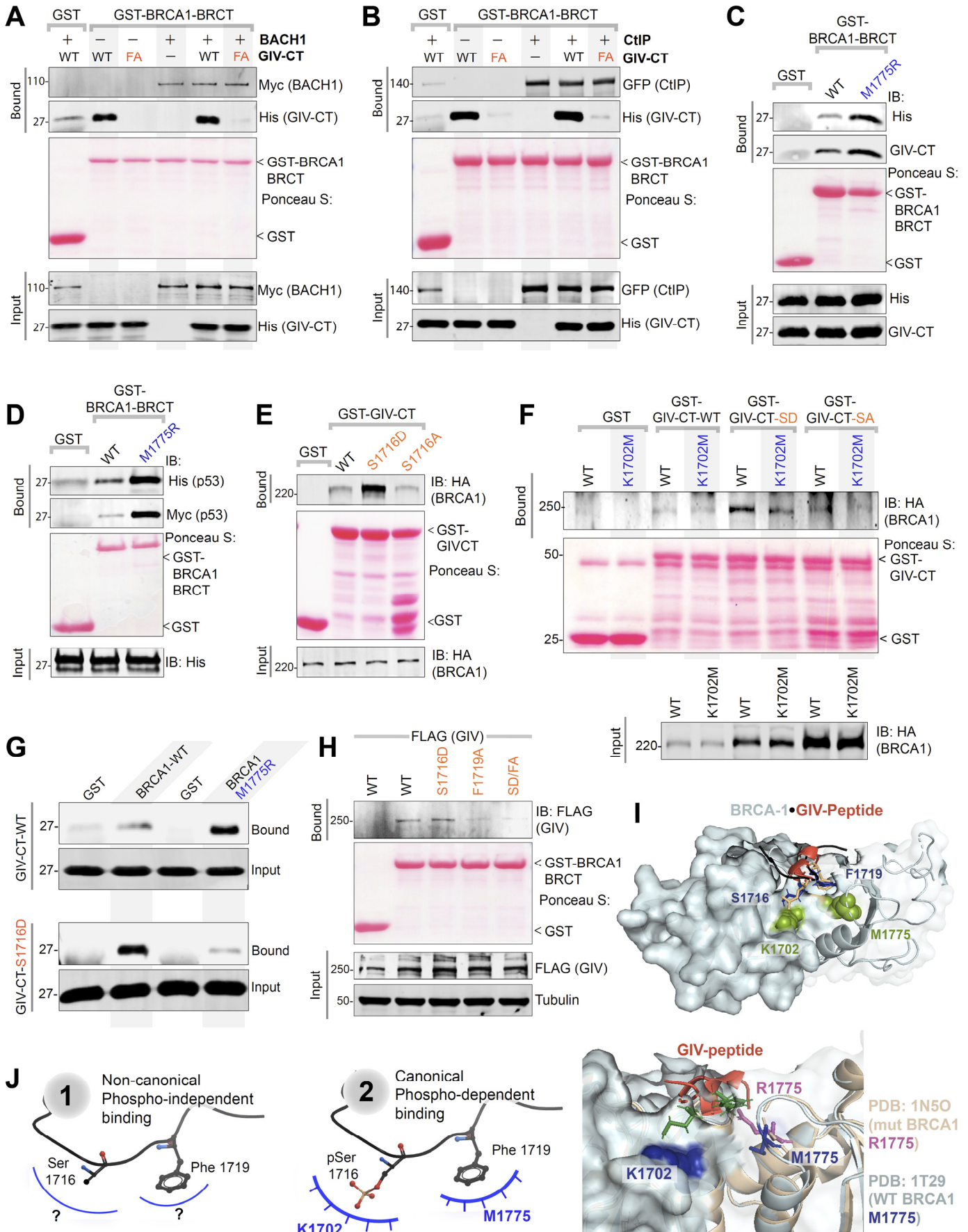
729 **A.** Schematic outlining key steps in BioID studies to identify the GIV interactome. **B.** Immunoblots confirm
730 biotinylation in HEK whole cell lysates (left) and expression of the BirA-tagged full-length GIV construct as a
731 protein of expected size (right). **C-D.** Bar plots show GO analyses [cellular component (C) and molecular function
732 (D)] for bioID-identified GIV interactome. Red bars in C indicate putative compartments where GIV binds BRCA1.
733 Blue and red bars in D indicate total number of interacting proteins and % representation, respectively. Red
734 arrow in D indicates the molecular function category where BRCA1 was identified. **E-F.** DNA-binding proteins
735 (listed in E) that were identified in GIV's interactome were analyzed by Reactome.org and visualized as
736 hierarchical reacfoam (in F). Inset in top right corner is magnified to highlight the overrepresentation of DNA
737 repair pathways.



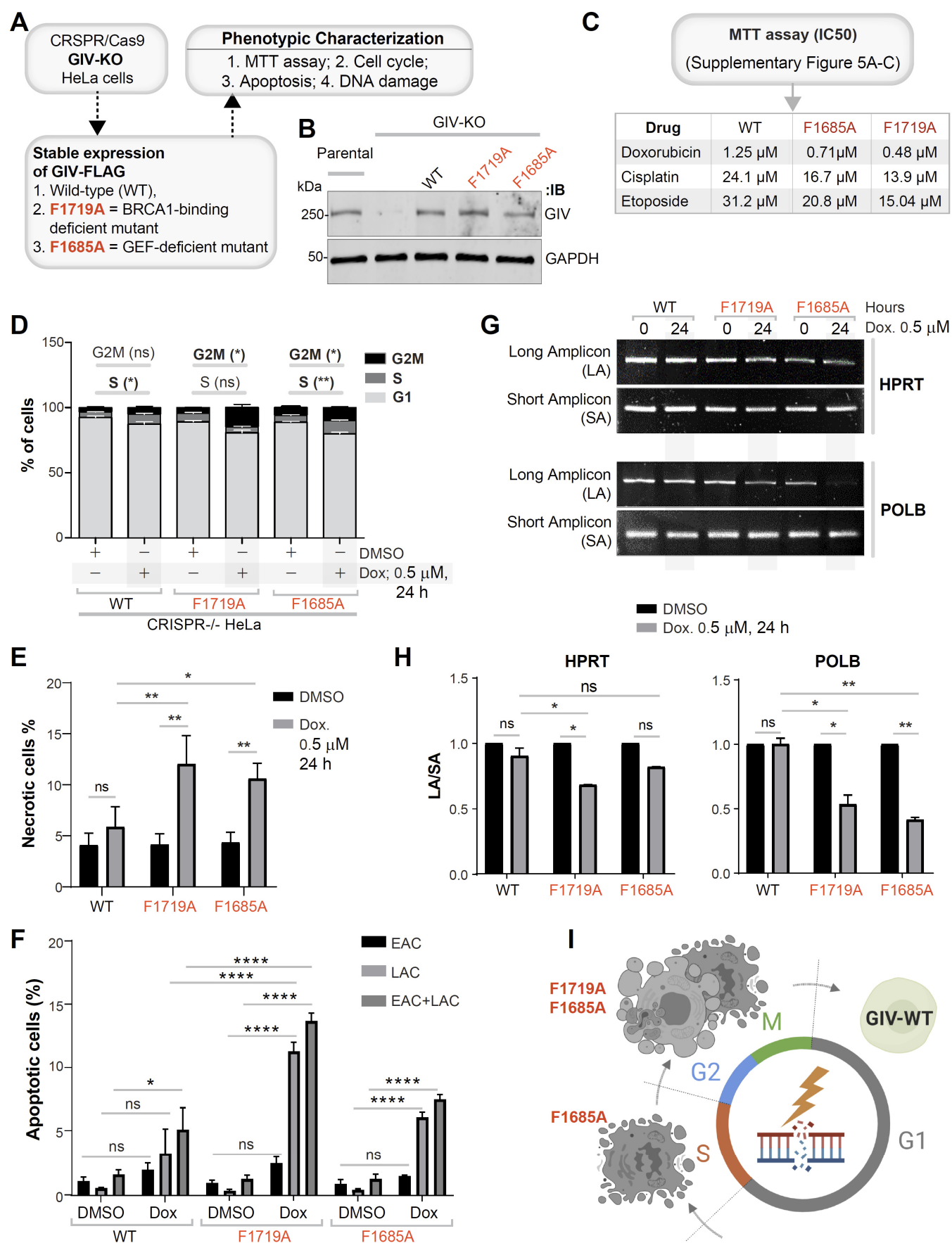
739 **Figure 2. DNA damage repair response is impaired in cells without GIV. A.** Schematic outlining the cell lines
740 and phenotypic assays displayed in this figure. **B.** Immunoblot of GIV-depleted (by CRISPR Cas9) and control
741 (Parental) HeLa cell lysates showing depletion of full-length endogenous GIV. See also Fig S1 for how pooled
742 KO lines were generated. **C.** Table of IC50 values for 3 different drugs tested on parental and GIV KO HeLa
743 cells, as determined using MTT assays. See **Fig S1C-E** for the dose-dependent survival curves. **D.** Stacked bar
744 graphs showing the percentage of cells at various stages of the cell cycle (G1, S and G2/M) after challenged
745 with Dox or vehicle control (DMSO). Histograms are shown in **Fig S1F**. Data displayed as mean \pm S.E.M. and
746 one-way ANOVA using Tukey's multiple comparisons test was used to determine significance. (*; $p \leq 0.05$, **; p
747 ≤ 0.01 ; ns = not significant). **E-F.** Bar graphs display the % necrotic (E) or apoptotic (early, EAC; late, LAC; or
748 combined) cells after challenged with either Dox or vehicle control (DMSO), as assessed by annexin V staining
749 and flow cytometry. See **Fig S1G** for the dot plot diagrams. **G-H.** Long amplicon qPCR (LA-QPCR) was used to
750 evaluate genomic DNA SB levels in control vs. GIV KO cells. Representative gel showing PCR-amplified
751 fragments of the *HPRT* (G, top panel) and *POLB* (G, bottom panel) genes. Amplification of each large fragment
752 (upper panels) was normalized to that of a small fragment of the corresponding gene (bottom panels) and the
753 data were expressed as lesion frequency/10 Kb DNA and displayed as bar graph in H. Full-length gels can be
754 seen in **Fig S1H**. Data displayed as mean \pm S.E.M. and one-way ANOVA to determine significance. (**; $p \leq 0.01$;
755 ****; $p \leq 0.0001$; ns = not significant). **I.** Schematic summarizing the findings in cells with (parental; GIV +) or
756 without GIV (GIV KO; GIV -).



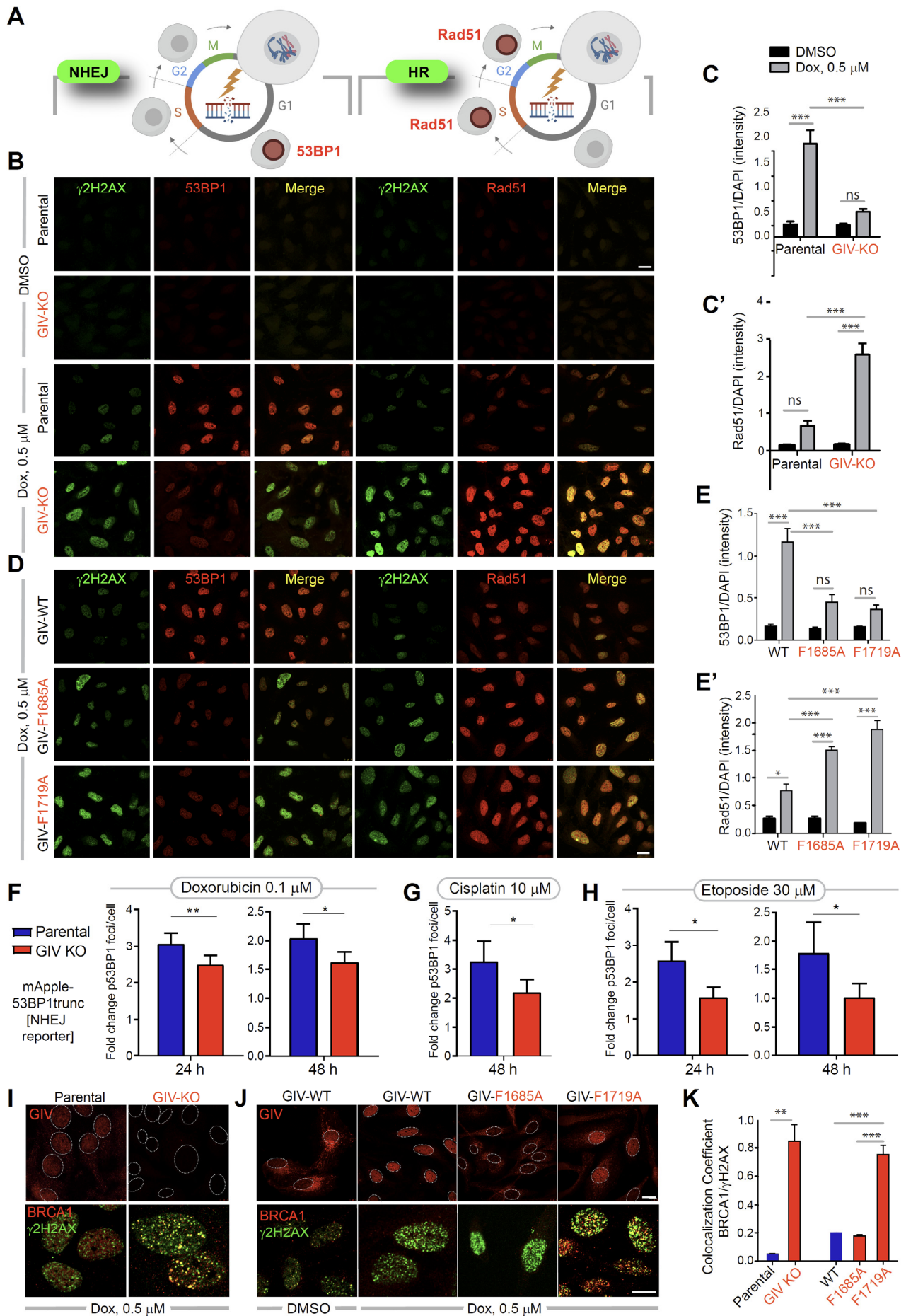
758
759 **Figure 3. GIV directly binds BRCT module of BRCA1 using a motif that is distinct from its G protein**
760 **regulatory motif. A.** Coimmunoprecipitation assays were carried out on lysates of HeLa cells using anti-BRCA1
761 antibody or control IgG and immune complexes (top) and lysates (bottom) were analyzed for GIV and BRCA1
762 by immunoblotting. **B.** Lysates of HEK cells exogenously expressing FLAG-tagged full-length GIV were used as
763 the source of GIV and BACH1 (positive control for known BRCA1-binding protein) in pulldown assays with GST-
764 tagged BRCA1 fragments and BRCT modules of various indicated proteins (visualized using Ponceau S). Bound
765 proteins (top) and lysates (bottom) were analyzed for GIV and BACH1. **C.** Pulldown assays were carried out
766 using recombinant His-GIV-CT (aa 1660-1870) and GST-BRCT modules as in B. Bound GIV was visualized by
767 immunoblotting (anti-His). **D.** Pulldown assays were carried out using lysates of HeLa cells as the source of
768 endogenous full-length GIV with GST-BRCA1 and BARD1. Bound GIV was visualized by immunoblotting. See
769 also **Fig S3** for similar studies with Cos7 and Hs578T cell lysates. **E-F.** Recombinant GIV-CT proteins of various
770 lengths (see schematic E) were used in pulldown assays with GST-BRCT module of BRCA1. Bound GIV-CT
771 fragments were analyzed in F by immunoblotting (His). **G.** Alignment of GIV's C-terminal sequence with known
772 phosphopeptides that bind BRCA1, as confirmed by x-ray crystallography (PDB codes on the left). The
773 consensus SxxF sequence is shown (evolutionary conservation of the SxxF motif and its relationship with other
774 motifs on GIV-CT is shown in **Fig S4**). **H.** Pulldown assays were carried out using His-GIV-CT WT or F1719A
775 mutant with GST/GST-BRCA1 and bound GIV was analyzed by immunoblotting. **I-J.** Pulldown assays were
776 carried out with either GDP-loaded GST-Gai3 (I) or GST-BRCA1 (BRCT; J) proteins and lysates of HEK cells
777 exogenously expressing FLAG-tagged GIV wild-type (WT) or GIV mutants that do not bind G protein (F1685A)
778 (20) or do not bind BRCA1 (F1719A; current work). Bound proteins were visualized by immunoblotting using
779 anti-FLAG IgG.



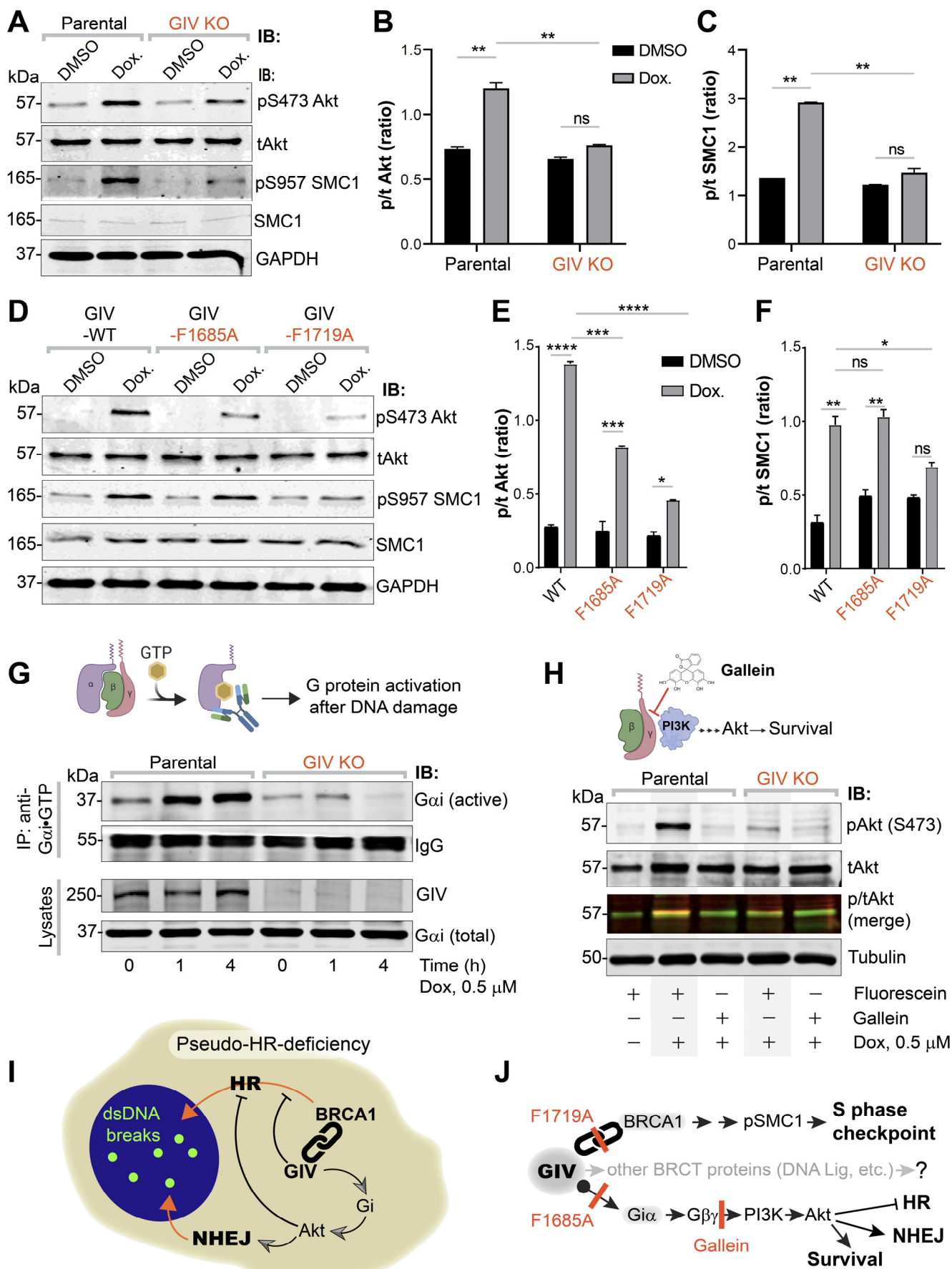
781 **Figure 4. GIV binds BRCA1 via both canonical (phosphodependent) and non-canonical**
782 **(phospho-independent) mechanisms. A-B.** Binding of unphosphorylated GIV with BRCA1 does not compete
783 with canonical, phospho-dependent binding of BACH1 (A) or CtIP (B). Pulldown assays were carried out using
784 lysates of HEK cells as source of myc-BACH1 (A) or GFP-CtIP (B) and recombinant GST/GST-BRCA1 proteins,
785 in the presence (+) or absence (-) of either wild-type (WT) or BRCA-binding deficient F1719A (FA) mutant His-
786 GIV-CT. Bound proteins were visualized by immunoblotting with anti-His (GIV), anti-myc (BACH1; A), or anti-
787 GFP (CtIP; B) IgGs. See also **Fig S5. C-D.** Pulldown assays were carried out using His-GIV-CT (C) or His-TP53
788 (D) and GST or GST-BRCA1 (WT and M1775R mutants). Bound proteins were visualized by immunoblotting
789 with anti-His IgG. **E.** Pulldown assays were carried out using lysates of HEK cells as the source of HA-BRCA1
790 (full length) with either GST (control) or wild-type (WT) and phosphomimic (S1716D) or non-phosphorylatable
791 (S1716A) mutant GST-GIV-CT. Bound BRCA1 was visualized by immunoblotting. **F.** Pulldown assays were
792 carried out as in E, using lysates of HEK cells exogenously expressing either wild-type (WT) or K1702M mutant
793 of HA-BRCA1. **G.** Pulldown assays were carried out using recombinant His-GIV-CT (WT or S1716D) and either
794 GST-BRCA1 WT or M1775R mutant protein as in C. Bound GIV was visualized by immunoblotting using anti-
795 His IgG. **H.** Lysates of HEK cells exogenously expressing full-length GIV-FLAG constructs were used as the
796 source of GIV in pulldown assays with GST/GST-BRCA1. Bound GIV was visualized using anti-FLAG IgG. **I.**
797 Homology model of phospho-dependent GIV•BRCA1 complex (I; *top*) built using the solved crystal structure of
798 BACH1•BRCA1 complex (PDB: IT29) as a template. GIV = red; major residues on BRCA1 or GIV that were
799 mutated here are labeled. Impact of M1775R mutant BRCA1 posing a steric clash with F1719 (GIV) is highlighted
800 (I; *bottom*). **J.** Schematic summarizing the two modes of binding of the same ¹⁷¹⁶SxxF¹⁷¹⁹ sequence on GIV-CT
801 to the BRCT module of BRCA1. The structural basis for phospho-independent binding remains unknown (*left*;
802 “?”).



804 **Figure 5. DNA damage repair response is impaired in cells expressing mutant GIV that cannot bind**
805 **BRCA1 (F1719A) or bind/activate G proteins (F1685A).** **A.** Schematic outlining the cell lines and phenotypic
806 assays displayed in this figure. **B.** Immunoblot of the HeLa cell lysates showing depletion of full-length
807 endogenous GIV, followed by rescue WT and mutant GIV at levels close to endogenous. **C.** Table of IC50 values
808 for 3 different drugs tested on parental and GIV KO HeLa cells, as determined using MTT assays. See **Fig S6A-**
809 **D** for the dose-dependent survival curves. **D.** Stacked bar graphs showing the percentage of cells at various
810 stages of cell cycle (G1, S and G2/M) after challenged with Dox or vehicle control (DMSO). Data displayed as
811 mean \pm S.E.M. and one-way ANOVA using Tukey's multiple comparisons test was used to determine
812 significance. (*; $p \leq 0.05$, **; $p \leq 0.01$; ns = not significant). Histograms are shown in **Fig S6E.** **E-F.** Bar graphs
813 display the % necrotic (E) or apoptotic (early, EAC; late, LAC; or combined) cells after challenge with either Dox
814 or vehicle control (DMSO) as assessed by annexin V staining and flow cytometry. See **Fig S6F** for the dot plot
815 diagrams. **G-H.** Long amplicon qPCR (LA-QPCR) was used to evaluate genomic DNA SB levels in various HeLa
816 cell lines. Representative gel showing PCR-amplified fragments of the *HPRT* (G, top panel) and *POLB* (G,
817 bottom panel) genes. Amplification of each large fragment (upper panels) was normalized to that of a small
818 fragment of the corresponding gene (bottom panels) and the data were expressed as lesion frequency/10 Kb
819 DNA and displayed as bar graph in H. Full length gels can be seen in **Fig S6G.** Data displayed as mean \pm S.E.M.
820 and one-way ANOVA to determine significance. (*; $p \leq 0.05$; ****; $p \leq 0.0001$; ns = not significant). **I.** Schematic
821 summarizing the findings in cells with GIV-WT or mutants that either cannot bind G protein (F1685A) or BRCA1
822 (F1719A).



824 **Figure 6. GIV inhibits HR, favors NHEJ, and inhibits localization of BRCA1 to sites of DNA damage.**
825 **A.** Schematic summarizing the two markers, 53BP1 (left) and Rad51 (right) commonly used to monitor repair
826 pathway of choice (NHEJ vs. HR, respectively) after DNA damage. **B-E'**. Control (parental) and GIV-depleted
827 (GIV KO) HeLa cells (B-C) or GIV-depleted HeLa cells stably expressing WT or mutant GIV constructs (D-E)
828 were challenged with Dox or vehicle control (DMSO) prior to being fixed and co-stained for γ H2AX (green) and
829 53BP1 (red; left) or Rad51 (red; right) and analyzed by confocal microscopy. Representative images are shown
830 in B and D (scale bar = 15 μ m). Bar graphs in C-C' and E-E' show the quantification of intensity of 53BP1 or
831 Rad51 staining normalized to DAPI. Data displayed as mean \pm S.E.M. and one-way ANOVA to determine
832 significance. (*; $p \leq 0.05$; **; $p \leq 0.01$; ***; $p \leq 0.001$; ns = not significant). **F-H.** Bar graphs display the fold change
833 in the number of bright foci of 53BP1 in parental and GIV KO HeLa cells stably expressing mApple-53BP1
834 reoprter (which detects NHEJ) upon challenge with the indicated concentrations of Doxorubicin (F), Cisplatin (G)
835 or Etoposide (H). Data displayed as mean \pm S.E.M. and t-test to determine significance. (*; $p \leq 0.05$; **; $p \leq$
836 0.01). See also **Fig S7A-B** for 53BP1 reporter studies on parental and GIV KO MDA-MB-231 cells. **I-K.** HeLa cell
837 lines in B, D were treated as in B, D, and fixed and analyzed for GIV (top) and BRCA1 (bottom) localization with
838 respect to the nuclei (demarcated with interrupted oval outlines). Representative images are shown in I-J (scale
839 bar = 15 μ m). See also **Fig S7B-C** for expanded individual panels. Bar graphs in K show Pearson's colocalization
840 coefficient for the degree of colocalization observed within the nucleus between BRCA1 (red) and γ H2AX (green).



842 **Figure 7. Activation of Gi by GIV is required for Akt enhancement during DDR, contributes to pseudo-**
843 **HR-deficiency. A-F.** Control (parental) and GIV-depleted (GIV KO) HeLa cells (A-C) or GIV-depleted cells stably
844 expressing WT or mutant GIV constructs (D-F) were challenged with Dox or vehicle control (DMSO) as indicated
845 prior to lysis. Equal aliquots of lysates were analyzed for total (t) and phosphorylated (p) Akt and SMC1 proteins
846 and GAPDH (loading control) by quantitative immunoblotting using LiCOR Odyssey. Representative
847 immunoblots are shown in A and D, and quantification of phospho(p)/total(t) proteins is displayed as bar graphs
848 in B, C, E, F. **G.** Schematic on top shows the assay used for assessing the extent of Gai-activation using
849 conformation-sensitive antibodies that selectively bind the GTP-bound (active) conformation of Gai protein.
850 Immunoblots below show the active Gai immunoprecipitated (top; IP) from lysates (bottom) of HeLa cells treated
851 with Dox. for the indicated time points. **H.** GIV-depleted (GIV KO) and control (Parental) HeLa cells were
852 stimulated (+) or not (-) with Dox. as indicated, in the presence of either Gallein or its inactive isomer, Fluorescein.
853 Equal aliquots of lysates were immunoblotted for pAkt and tAkt as in panel A. I-J. Summary of findings showing
854 how GIV skews the choice of repair pathway from HR to NHEJ, partly via sequestration of BRCA1 away from
855 the sites of dsDNA breaks and in part via the enhancement of Akt via the Gi→'free' Gβγ→Class I PI3K pathway.
856 The tools (mutants and chemical inhibitors) used in this work are highlighted in red.